Summer 6-2014

ORIGIN AND DISTRIBUTION OF THE MISSISSIPPIAN – PENNSYLVANIAN BOUNDARY UNCONFORMITY IN MARINE CARBONATE SUCCESSIONS WITH A CASE STUDY OF THE KARST DEVELOPMENT ATOP THE MADISON FORMATION IN THE BIGHORN BASIN, WYOMING.

Lucien Nana Yobo
University of Nebraska-Lincoln, nanalucien@huskers.unl.edu

ORIGIN AND DISTRIBUTION OF THE MISSISSIPPIAN – PENNSYLVANIAN BOUNDARY UNCONFORMITY IN MARINE CARBONATE SUCCESSIONS WITH A CASE STUDY OF THE KARST DEVELOPMENT ATOP THE MADISON FORMATION IN THE BIGHORN BASIN, WYOMING.

By

Luscalors Lucien Nana Yobo

A THESIS

Presented to the Faculty of

The Graduate College at the University of Nebraska

In Partial Fulfillment of Requirements

For the Degree of Master of Science

Major: Earth and Atmospheric Sciences

Under the Supervision of Professor Tracy D. Frank

Lincoln, Nebraska

June, 2014

ORIGIN AND DISTRIBUTION OF THE MISSISSIPPIAN – PENNSYLVANIAN BOUNDARY UNCONFORMITY IN MARINE CARBONATE SUCCESSIONS WITH A CASE STUDY OF THE KARST DEVELOPMENT ATOP THE MADISON FORMATION IN BIG HORN BASIN, WYOMING.

Lucien Nana Yobo, MS

University of Nebraska, 2014

Advisor: Tracy D. Frank

The causal mechanism of the widespread unconformity that encompasses the Mississippian – Pennsylvanian boundary remains poorly understood. This unconformity, first thought to be restricted to North America, is now known to be present in other regions of the globe. Possible causes for the unconformity include (1) sea level draw down from the onset of glaciation at start of the late Paleozoic ice age and (2) increased tectonic activity from the formation of the supercontinent of Pangea. Thus the origin of the unconformity is still poorly constrained.

This study examines possible causal mechanisms for the widespread unconformity that encompasses the Mississippian – Pennsylvanian boundary through examination of published stratigraphic records from nine paleotropical sites as well as field study of the karst development on top of the Madison Formation formed at the unconformity interval as an outcrop analog for examination of key reservoir properties to aid in the assessment of equivalents in the subsurface. The nine paleotropical sites looked at included, 1) Arrow Canyon, NV, USA, 2) U.S. Midcontinent, 3) Madison Platform, Big Horn Basin, WY, USA 4) Bechar Basin, Algeria, 5) Palentian Zone, Cantabrian

Mountains, Northwest Spain, 6) Central Taurides, Turkey, 7) Donets Basin, Ukraine, 8) Southern Ural Mountains, Russia and 9) South China Platform.

Results from the sites show the development of a sequence boundary and or a shallowing of facies across the boundary, such global synchroneity of stratigraphic patterns suggests that the unconformity encompassing the Mississippian – Pennsylvanian boundary was as a result of global eustatic fall consistent with ice buildup at the onset of the late Paleozoic ice age. Additionally, in areas where tectonism was prevalent, eustatic signals were masked. Also, the heterogeneity and spatial complexes formed as a result of the karst development on at the Mississippian – Pennsylvanian boundary in the Madison Formation of Bighorn Basin Wyoming have shown to be consistent with subsurface examples in China, thus suggesting the viability of the Madison paleokarst as an outcrop analog. Finally, since this interval serves as hydrocarbon reservoir in some parts of the US Midcontinent and the Rocky Mountain region, proper understanding of the widespread distribution of the unconformity as well as reconstruction of the karst feature developed at the Mississippian – Pennsylvanian boundary will aid in global exploration of hydrocarbon.

DEDICATION

To my parents Abraham and Florence.

ACKNOWLEDGMENTS

The completion of this thesis would not have been possible if not for the following individuals. I am forever indebted and would like to express my sincerest gratitude towards the following individuals and organizations: first and foremost, my advisor Dr. Tracy D. Frank for her understanding, flexibility and her immeasurable assistance and mentorship during the completion of this project. Thank you for your continued support and encouragement for I have grown and learned a lot under your tutelage. Secondly, the University of Nebraska-Lincoln Department of Earth and Atmospheric Sciences for offering me the opportunity to conduct graduate level research. I would like to thank my parents Abraham and Florence, my sisters Lauritta, Larissa and Vanessa for their support and encouragement as well as my friends in the department, UNL and Lincoln for making my Lincoln experience wonderful. Additionally, I'd like to thank Dr. Caroline Burberry and Dr. Christopher R. Fielding for serving on my committee.

Finally, this project wouldn't have been possible were it not for funding from NSF CAREER Grant EAR-0645504 to T. Frank, and a Geological Society of America student grant to L. Nana Yobo.

TABLE OF CONTENTS

CHAPTER TITLE/ SECTION PG.

LIST OF FIGURES

CHAPTER FIGURES

LIST OF TABLES

CHAPTER TABLE

THESIS STRUCTURE

This thesis is organized as a series of two manuscripts separated into two chapter formats that would be submitted for publication. The first chapter focuses on understanding the origin of the Mississippian – Pennsylvanian boundary unconformity in marine carbonate successions, from nine paleotropical regions, while the second chapter focuses on understanding the regional karst development formed at the Mississippian – Pennsylvanian boundary in the Madison Formation.

CHAPTER ONE

ORIGIN AND DISTRIBUTION OF THE MISSISSIPPIAN-PENNSYLVANIAN BOUNDARY UNCONFORMITY IN MARINE CARBONATE SUCCESSIONS.

ABSTRACT

The causal mechanism of the widespread unconformity that encompasses the Mississippian – Pennsylvanian boundary remains poorly understood. This unconformity, first thought to be restricted to North America, has now been shown to be present in other regions of the globe. Possible causes for the unconformity include (1) sea level draw down from the onset of glaciation at start of the late Paleozoic ice age and (2) increased tectonic activity from the formation of the supercontinent of Pangea. Thus the origin of the unconformity is still poorly constrained.

This study examines causal mechanisms for the widespread unconformity developed across the Mississippian – Pennsylvanian boundary interval through examination of published stratigraphic records from nine paleotropical sites where shallow marine carbonate accumulated. Shallow marine carbonates are used because they are sensitive to changes in sea level. Sites include 1) Arrow Canyon, NV, USA, 2) U.S. Midcontinent, 3) Madison Platform, Big Horn Basin, WY, USA 4) Bechar Basin, Algeria, 5) Palentian Zone, Cantabrian Mountains, Northwest Spain, 6) Central Taurides, Turkey, 7) Donets Basin, Ukraine, 8) Southern Ural Mountains, Russia and 9) South China Platform. The compiled stratigraphic data are calibrated against the latest biostratigraphic and absolute time constraints available so as to estimate the onset and duration of the unconformity. Results show the development of a sequence boundary and

or abrupt shallowing of facies across the interval in all the sites examined for this study. These relationships suggest that the unconformity evident here was formed as a result of sea level drawdown during the Serpukhovian – Bashkirian, consistent with ice buildup during onset of the late Paleozoic ice age. Additionally, prevalent tectonism active during the period may have been overprinted or masked by the sea level drawdown, thereby making the unconformity of longer duration in some regions than others. The unconformity is highly variable and represents 1 – 34 m.y of non-deposition. Understanding the widespread distribution of the unconformity can be used as a predictive tool in global hydrocarbon exploration since the interval already serves as a major hydrocarbon reservoir in some parts of the United States Midcontinent, U.S Rocky Mountain region and Canada.

INTRODUCTION

The Mississippian-Pennsylvanian boundary in Euramerica often occurs as an unconformity. This unconformity was previously thought of as a North American phenomenon, that is, it was assumed to be evident only in North America. However, Saunders and Ramsbottom (1986) showed using both stratigraphic evidence and fossil group assemblages that the unconformity was not just restricted to North America, but has a broader distribution globally. In light of this, a global phenomenon would be most likely responsible for the unconformity. The timing of the unconformity coincides with the start of the Late Paleozoic ice age (Isbell et al., 2003; Fielding et al., 2008a), which may have affected global sea level, as well as continental collision during the assembly of supercontinent of Pangea (Blakey, 2008 and references therein).

As a result, the origin of the unconformity, whether tectonic or eustatic or otherwise and to what extent each had on the formation of the unconformity, is still highly contentious. For example, using lithospheric flexural stratigraphy, Beuthin (1994) showed that the unconformity in the Appalachian Basin postdated the boundary, while Ettensohn (1980) demonstrated that the Mississippian – Pennsylvanian unconformity in northeastern Kentucky was a result of syn-sedimentary tectonic activity. These studies suggest regional factors may be responsible for the unconformity, at least in part. If the unconformity evident in the Mississippian – Pennsylvanian boundary was formed from draw down of sea level as a result of the onset of Gondwana glaciation, then significant exposure events should be recorded across the Mississippian – Pennsylvanian interval worldwide. However, if it was formed as a result of tectonic activity, then its expression should vary locally. Shallow water carbonate platforms and ramps are used for this study because carbonate deposits are sensitive to fluctuations in sea level.

This study examined stratigraphic record from nine marine carbonate successions based on available literature (Fig 1.), sites include 1) Arrow Canyon, NV, USA, 2) U.S. Midcontinent, 3) Madison Platform, Big Horn Basin, WY, USA 4) Bechar Basin, Algeria, 5) Palentian Zone, Cantabrian Mountains, Northwest Spain, 6) Central Taurides, Turkey, 7) Donets Basin, Ukraine, 8) Southern Ural Mountains, Russia and 9) South China Platform. The stratigraphic records were analyzed to determine the expression timing, and duration of the unconformity where present. Results are used to assess the principal cause of the unconformity i.e. tectonism, sea level drawdown or both, to improve our understanding of the expression of the unconformity that encompasses the Mississippian - Pennsylvanian boundary.

BACKGROUND

An unconformity is a break or a period of non-deposition of sediments; this break often leads to the formation of an erosional surface. Identification of unconformable surfaces is aided by presence of features that record subaerial exposure (e.g. root structures, paleokarst features and paleosol horizons) or non depositional (hardgrounds). Unconformities can be formed by a change in base level due to, for example, drawdown of sea level, or by a number of other processes. Thus, to understand the nature of the unconformity that encompasses the Mississippian – Pennsylvanian boundary, knowledge of late Paleozoic events that may have affected sea level, climate, and the nature of deposition are necessary.

The Mississippian – Pennsylvanian period records a major climatic transition from greenhouse to icehouse conditions (Bishop et al., 2009). Studies from glaciogenic sediments, geochemical records and cyclotherm stacking patterns have yielded increase understanding and timing of this major climate transitions (e.g. Bishop et al., 2009; Mii et al., 1999; Mii et al., 2000; Isbell et al., 2003). These studies have estimated the onset of the late Paleozoic ice age to range from early Visean to mid-Carboniferous (Veevers and Powell, 1987; Isbell et al. 2003; Bishop et al., 2009; Fielding et al., 2008). On the other hand chemostratigraphic studies have also shown variable estimates from Visean – mid-Serpukhovian for the onset of the LPIA (Brunschen et al., 1999; Bishop et al., 2009). These slight discrepancies in timing of the onset have been attributed to sedimentary processes and glacial advances (Bishop et al., 2009).

The LPIA was first thought of as a single event that covered much of Gondwana and lasted from the Middle to Late Mississippian to Early Permian (Veevers and Powell, 1987). Studies across Gondwana by Isbell et al. (2003) challenged this view and divided the LPIA into three distinct periods of glaciations separated by periods of non-glacial conditions. However, Fielding et al. (2008a) from work in eastern Australia resolved the LPIA, dividing it into eight distinct glacial intervals separated by periods of non-glacial condition, four in the Carboniferous and four in the Permian, with each lasting about 1 - 8 m.y. These four Carboniferous glacial intervals are numbered C1-C4; C1 – basal Serpukhovian, C2 – latest Serpukhovian to Earliest Bashkirian, C3 – middle Bashkirian and C4 – late Bashkirian to middle Moscovian (Fielding et al., 2008a). The duration of glaciation was not all equal; for example, the C1 glaciation lasted for about 1 m.y. while the C2 glaciation lasted for about 3.5 m.y. (Fielding et al., 2008a).

The notion of glacial expansion at the Serpukhovian – Bashkirian boundary is also supported by stable isotopic values, which show positive excursions in $\delta^{13}C$ and $\delta^{18}O$ values of marine carbonates, consistent with a decrease in atmospheric pCO_2 and an increase in ice volume as global climate cooled and glaciers expanded, and is coincident with the C2 glacial interval. (Mii et al. 1999; Fielding et al., 2008b; Frank et al. 2008).

At the same time, the Late Paleozoic was a time of increased tectonic activity from the formation of the supercontinent of Pangea (Scotese and Langford, 1995; Blakey, 2008), that began with the collision of western Africa and eastern North America, generating the Alleghanian orogeny and resulting in the Variscan-Appalachian mountain chain (Blakey, 2008). This could have aided in the formation of an unconformity at the Mississippian - Pennsylvanian boundary.

Because the mid-Carboniferous was characterized by high amplitude sea level oscillations (Ross and Ross, 1985; Wright and Vanstone, 2001; Rygel et al., 2008), attempts at resolving the cause of the Mississippian – Pennsylvanian unconformity have applied sequence stratigraphy to generate glacio-eustatic curves for the interval (Saunders and Ramsbotton, 1986; Miller and Eriksson, 2000; Waters and Condon, 2012). However, since the boundary is not everywhere coincident with a subaerial exposure surface, placement of the boundary to correspond with a sequence boundary has yielded many discrepancies (Barnet and Wright, 2008; Atakul-Ozdemir et al., 2011).

METHODS

This study makes use of published stratigraphic data from carbonate ramps and platforms across low latitude regions of Gondwana and Euramerica and focuses primarily on sources that have complete stratigraphic records and a well-defined chronostratigraphic framework that can be used for correlation with other basins/regions. Carbonate were chosen for this study because carbonate deposits are sensitive to fluctuations in climate, oceanography, and sea level thus providing an ideal means of investigating the effect of glacial activity. In addition, carbon isotope stratigraphy of marine carbonate successions record climatic changes that result from fluctuations in the global carbon cycle. These fluctuations can be traced globally and are used to understand changes in the global climate and atmospheric pCO_2 (Frank et al., 2008).

Owing to the extensive global tectonic activity prevalent during this time, most of the sites chosen for this study were tectonically quiescent with the exception of the Central Taurides (Turkey), which was actively subsiding (Atakul-Ozdemir et al., 2010).

Thus at this site the effect of sea level lowering may have been masked by subsidence. However, this area was included so as to understand how tectonics might have affected the expression of the unconformity that encompasses the Mississippian – Pennsylvanian boundary and because the region has a continuous section through the mid-Carboniferous interval as well as finely resolved biostratigraphic data and well understood stratigraphy. Tectonically quiet sites were chosen for this study so as to avoid any tectonic interference and if the unconformity recorded at this interval is present in tectonically quiet areas, then it would suggest a eustatic change as the most likely cause for the unconformity that encompasses the Mississippian – Pennsylvanian interval.

These stratigraphic data (lithology/facies, locations of unconformity, duration of hiatus, and paleogeographic locations) from nine different regions were compiled (see Table 1 for summary of stratigraphic data) and calibrated with the most recent geologic time scale of Gradstein et al. (2012; Fig. 2). These stratigraphic data were then compared with the timing of Gondwana glacial epoch from Fielding et al. (2008a), as well as stable isotope data from Frank et al. (2008). This produced a framework to allow for easy comparison with the various data (Fig. 3).

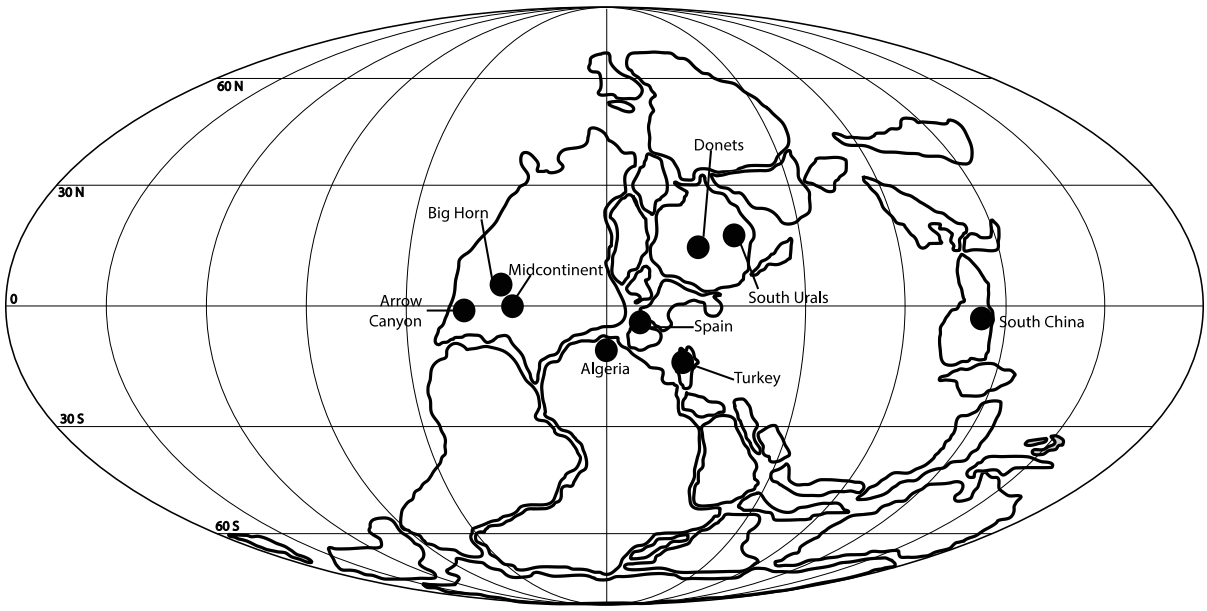

Fig. 1: Location map of stratigraphic sections used in this study. Continental reconstruction for Late Carboniferous from Golonka and Ford (2000).

Biostratigraphic correlation

Biostratigraphic resolution varies from region to region, however, conodonts, foraminifera, ammonoids and some fusulinids are most commonly used for correlation. Gradstein et al. (2012) provides the most recent global biostratigraphic framework for this interval (Fig. 2).

Conodonts

Conodonts are the most used index fossil for correlation of successions across the Mississippian – Pennsylvanian boundary. The Mississippian-Pennsylvanian boundary correlations were made based on the GSSP for the base of the Pennsylvanian (Lower Bashkirian), which has been fixed in Arrow Canyon, Great Basin, Nevada, USA (Lane et al., 1999). This boundary corresponds to the first appearance datum (FAD) of conodont *Declinognathodus noduliferus s.l.* (Lane et al., 1999). A polyphyletic origin has been suggested for *D. noduliferus* so as to settle some potential discrepancies of its evolution in the eastern and western hemisphere sections (Gradstein et al., 2012 and references therein). In the Cantabrian Mountains of northwest Spain, the *D. noduliferus bernesgae* is found in sections dated with conodonts and ammonoids as Serpukhovian (Sanz-Lopez et al., 2006).

Foraminifera

Foraminifera are also widely used as a biostratigraphic tool for the correlation of mid-Carboniferous sections. The foraminifer *Globivalvulina bulloides* has been used to identify the Mississippian - Pennsylvanian boundary (Brenckle et al., 1997). However in the Donets Basin of Ukraine, this foraminifer occurs slightly below the boundary, thus

foraminifer *Milleralla pressa and M. Marblensis* are also designated as informal markers for the boundary (Brenckle et al., 1997).

Ammonoids

Ammonoids are also used as biostratigraphic markers for sections of the mid-Carboniferous interval. The Mississippian - Pennsylvanian boundary is marked at the base of ammonoid zone *Homoceras or Isohomoceras subglobosum* (Ramsbottom and Saunders, 1985).

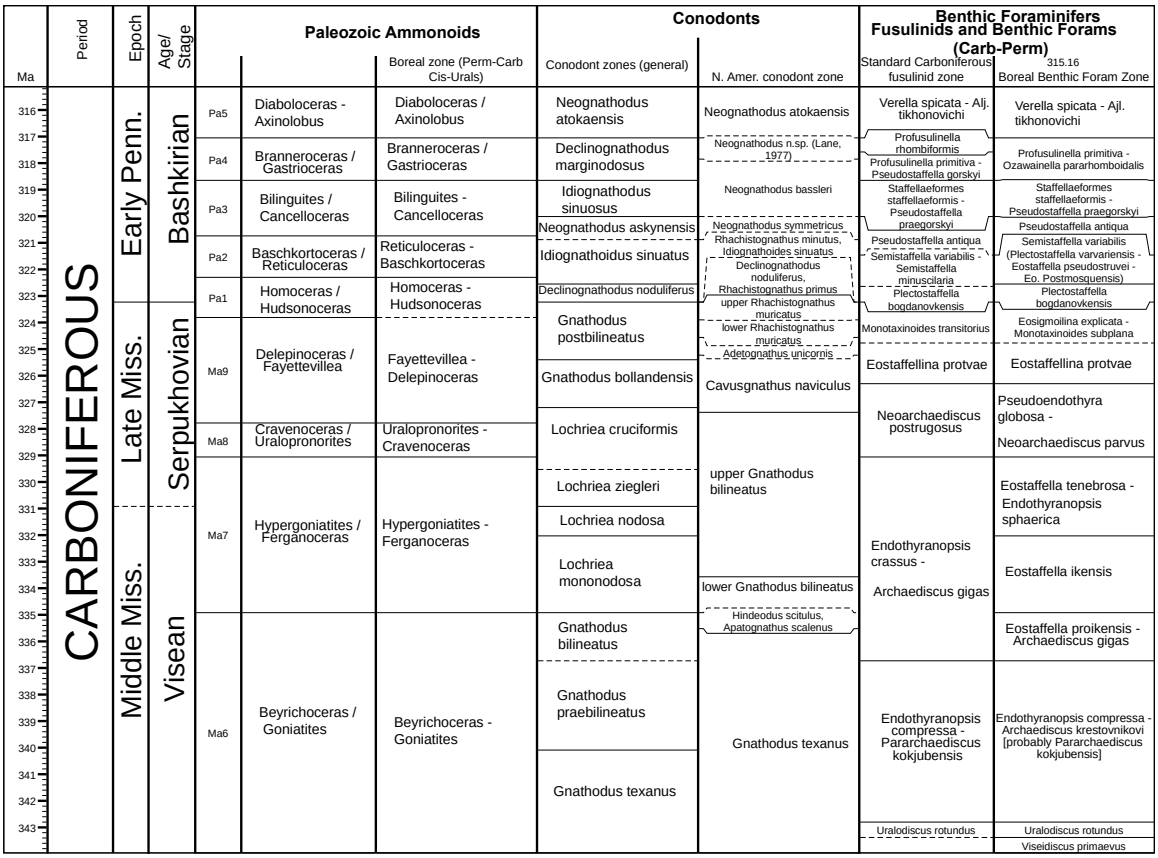

Fig. 2: Biostratigraphic data from Gradstein et al. (2012 and references therein) used for age calibration.

Table 1: Summary of Stratigraphic data from locations examined.

Region	**Formation Studied**	**Paleolatitude (**Scotese and McKerrow, 1990; Blakey, 2008; Golonka and Ford, 2000)	**Nature of mid-Carboniferous boundary**	**Primary age control**	**Duration of Unconformity**	**Key references**
Arrow Canyon	Indian Springs and Bird Spring Formation	0 – 5° S	Conformable, however subaerial exposure surfaces is occur above and below the boundary	Conodonts, ammonoids,	Conformable, however, duration of subaerial exposure surfaces is about 10^3-10^5 years.	Lane et al., 1999; Richards et al., 2002, Barnett and Wright 2008; Bishop et al., 2009.
Donets	D^8_5 limestone	10 – 15° N	Conformable through the upper D^8_5 limestone.	Conodonts, foraminifera, ammonoids, brachiopods, and U-Pb ages		Skipp et al., 1989; Davydov et al., 2010; Eros et al, 2012; Ogar, 2012
South China	Hezhou, Laobadong and Huanglong	0 – 15 S	Regional disconformity or major facies change.	Conodonts, foraminifers, ammonoids and fusulinids.		Zhi, 1985; Zhihao et al., 1987; Zhihao and Yuping, 2003; Ueno et al., 2012; Wang et al., 2013
Algeria	Djenien and Tagnana Formation	10° - 15°	Boundary is conformable, however, missing biostratigraphic taxa suggests a hiatus.	Conodonts, corals, foraminifera and ammonoids	Missing biostratigraphic taxa suggests a hiatus of 1 m.y	Pareyen, 1961; Bishop, 1975; Lemosquet and Pareyen, 1982; Manger et al., 1985; Sabbar and Ouali, 1996; Madi et al., 2000.
US Midcontinent	Piktin Limestone and Hale Formation	0 – 10° N	Expressed regional as an unconformity.	Conodonts, ammonoids and $^{40}Ar/^{39}Ar$ dates	About 5 m.y.	Lane and De Keyser, 1980; Newell et al., 1987Manger and Sutherland, 1992; Webb, 1994; Groves et al., 1999;
South	Bukharcha	15 – 25° N	Conformable but some	Conodonts,	Hiatus of about 1 m.y	Sinitsyna et al.,

Urals	Formation		isotopic and biostratigraphic evidence suggests a hiatus across the boundary in the Askyn River section.	foraminifera, ammonoids and U-Pb dates	at the Askyn River section.	1995; Proust et al., 1998; Groves et al., 1999; Brand and Bruckschen, 2002; Kulagina et al., 2013;
Big Horn Basin	Madison Formation	5˚ N	Regional unconformity	Conodonts	10 m.y up to about 34 m.y	Sando, 1985, 1988; Sonnenfeld, 1996a,b.
Central Taurides (Turkey)	Yaricak Formation	10 – 20° S	Conformable in the Lower member of the Yaricak Formation, but records a shallow upward of facies across the boundary.	Conodonts and foraminifera		Yilmaz and Altiner, 2006; Atakul-Ozdemir et al., 2011, 2012
Spain (North Cantabrian mountains)	Barcaliente Formation	5 – 15° S	Conformable in the Lower member of the Barcaliente Formation.	Conodonts, and foraminifera		Hemleben and Reuther, 1980; Sanz-Lopez et al., 2006; Nemyrovska et al., 2008, 2011;

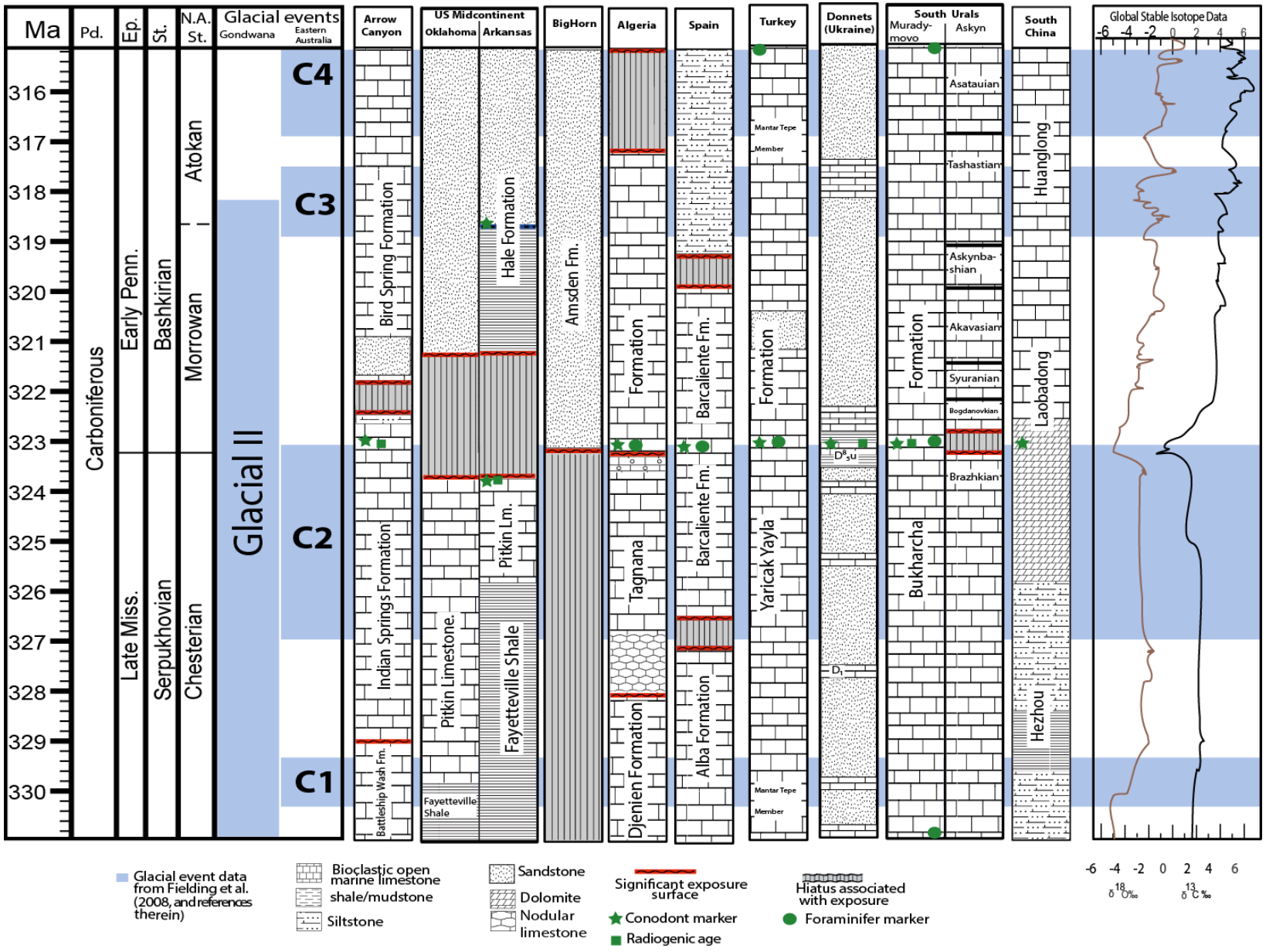
Ma
Pd.
Ep.
St.
N.A. St.
Glacial events
Gondwana
Eastern Australia
Carboniferous
Early Penn.
Late Miss.
Bashkirian
Serpukhovian
Morrowan
Chesterian
Atokan
Glacial II
C4
C3
C2
C1
316
317
318
319
320
321
322
323
324
325
326
327
328
329
330
Arrow Canyon
Bird Spring Formation
Indian Springs Formation
Battleship Wash Fm.
US Midcontinent
Oklahoma
Arkansas
Hale Formation
Pitkin Lm.
Pitkin Limestone.
Fayetteville Shale
Fayetteville Shale
BigHorn
Amsden Fm.
Algeria
Formation
Tagnana
Djenien Formation
Spain
Barcaliente Fm.
Barcaliente Fm.
Alba Formation
Turkey
Mantar Tepe Member
Formation
Yaricak Yayla
Mantar Tepe Member
Donnets (Ukraine)
D8su
D1
South Urals
Murady-movo
Askyn
Asatauian
Tashastian
Askynba-shian
Akavasian
Syuranian
Bogdanovkian
Brazhkian
Formation
Bukharcha
South China
Huanglong
Laobadong
Hezhou
Global Stable Isotope Data
-6 -4 -2 0 2 4 6
Glacial event data from Fielding et al. (2008, and references therein)
Bioclastic open marine limestone
shale/mudstone
Siltstone
Sandstone
Dolomite
Nodular limestone
Significant exposure surface
Conodont marker
Radiogenic age
Hiatus associated with exposure
Foraminifer marker
-6 -4 -2 0 2 4 6
δ 18O‰
δ 13C ‰

Fig 3. Chronostratigraphic framework of the nine regions reviewed for this study. Stratigraphic data for each section are compiled from references in Table 1, while isotope date are complied from Frank et al. (2008). Lithology symbols are included at the base of the figure. Red horizontal line/shading represents unconformity associated with significant exposure. Key conodont, foraminifera and absolute ages used for correlation are denoted by stars, circles and square respectively.

STRATIGRAPHIC RECORDS

United States

Arrow Canyon, Great Basin Nevada, USA.

Arrow Canyon, located in Great Basin of Southwestern Nevada, USA, is about 75 miles NE of Las Vegas, NV, and was part of the tropical to subtropical interior seaway "Cordilleran Miogeosyncline" that extended from Canada through Montana and Idaho to southern California and (Ross 1979). During the Carboniferous, it was located between 0 – 5° S of the equator, near the Panthalassan margin of North America (Blakey, 2008). This setting allowed for the basin to be flooded by a shallow sea, depositing carbonates (Poole and Sandberg, 1991). The Carboniferous strata here are made up of the Yellow-Pine Formation (Visean), the Battleship Wash Formation (Latest Visean – Early Serpukhovian) Indian Springs Formation (Serpukhovian) and the Bird Spring Formation (Late Serpukhovian – Bashkirian) (Fig. 3).

Robust biostratigraphic control (e.g. Pierce and Langenheim, 1972; Poole and Sandberg 1991; Brenckle et al., 1997; Lane et al., 1999) makes it ideal for studying the Mississippian - Pennsylvanian boundary interval. It serves as the Global Boundary

Stratotype and Point (GSSP), approved by the International Commission on Stratigraphy (ICS) and ratified by the International Union of Geological sciences (IUGS)(Lane et al., 1999).

The Mississippian - Pennsylvanian boundary interval in Arrow Canyon is presumed complete and not marked by unconformity or hiatus. The boundary is placed in the Lower Bird Spring Formation (a carbonate dominated succession) and was considered by Lane et al. (1999), who described the succession to be continuous and presumed complete both lithologically and biostratigraphically.

The Mississippian – Pennsylvanian boundary interval is marked by a facies change from a crinoidal packstone-grainstone and cross-laminated sandy bioclastic grainstone below the boundary, to fossiliferous low angle planar cross-bedded quartz arenite sandstone above the boundary (Barnett and Wright 2008; Bishop et al., 2009).

United States Midcontinent

The U.S. Midcontinent, here represented by deposits in Oklahoma and Arkansas, was located between 0 – 10° N during the Carboniferous (Golonka and Ford, 2000). During this time, the area was tectonically stable and this setting allowed for development of a large carbonate platform and deposition of laterally extensive and continuous carbonates and siliciclastics (Lane and De Keyser, 1980; Newell et al., 1987). Age control of the strata is made through conodont biostratigraphy as well as $^{40}Ar/^{39}Ar$ dating, allowing for well-constrained stratigraphic records across the mid-Carboniferous boundary interval, (e.g. Manger and Sutherland, 1992; Groves et al., 1999) making it possible for correlation with other regions.

In the US midcontinent, the Mississippian - Pennsylvanian boundary interval occurs as a regional erosional unconformity between the Pitkin Limestone and the Cane Hill Member of the Hale Formation (a shallow tidal succession of siltstone, sandstone and shales) (Manger and Sutherland, 1992; Webb, 1994; Fig. 3), interpreted to indicate a major regional withdrawal of the sea level (Sutherland, 1988). In some places, the boundary interval is marked by an angular unconformity, which has been attributed to tectonic activity from the upwarping of the Ozark dome and a southward tilt of the Arkoma shelf (Sutherland, 1988).

In parts of Oklahoma, the unconformity that encompasses the Mississippian – Pennsylvanian boundary is marked by the presence of paleokarst and paleosols (including calcrete) which records maximum regression (Webb, 1994) and an estimated hiatus of about 5 m.y. Additional the unconformity surface exhibits a local topographic relief of more than 24 m (Sutherland and Henry, 1977).

In Arkansas, although discontinuous locally, a transgressive rocky shore deposit occurs at the base of the Lower Pennsylvanian Cane Hill Member of the Hale Formation (Johnson, 1988; Webb, 1994) overlying the Mississippian Pitkin Formation. This deposit is made up of rounded to sub-rounded clasts of the Pitkin Formation, as well as phosphate pebbles affected by borers and encrusters (Webb, 1994). The presence of the rocky shore deposits at the base of the Cane Hill Member is interpreted to be consistent with a sea level transgression (Webb, 1994).

Bighorn Basin WY, USA.

The Madison Platform was located at about 5˚ N during the Carboniferous

(McKerrow and Scotese, 1990) and extended for 1600km from Canada south into New Mexico and Arizona (Sando, 1988). The Madison Limestones were deposited from Kinderhookian to Early Meramecian stages (Sando, 1988) on a broad epeiric platform (Gutshick and Sandberg, 1983). The platform was bounded to the north by the central Montana trough and the Williston Basin, to the southeast by the transcontinental arch, and to the west by the Antler trough (Gutshick and Sandberg, 1983; Sonnenfield, 1996).

The Carboniferous strata of the Bighorn Basin are made up of the Mississippian Madison Formation and the Amsden (Lower Pennsylvanian) and Tensleep (Upper Pennsylvanian) Formation. The Mississippian Madison Formation accumulated in an open to restricted marine environment and is made up of two members; a lower limestone member termed The Lodgepole Limestone and an upper limestone member Mission Canyon Limestone. These members are unconformably overlain by the Darwin Sandstone of the Amsden Formation (Sando, 1988; Sonnenfeld, 1996; Fig. 3). Of all the sites examined in this study, the Madison Formation in the Bighorn Basin has the fewest biostratigraphic constraints.

The Mississippian – Pennsylvanian boundary interval in the Bighorn Basin is marked by an erosional unconformity that separates the upper Member of the Mississippian Madison Formation limestones from the Pennsylvanian Amsden Formation siliciclastics (Sando, 1988; Sonnefeld, 1996; Fig. 3). The time gap of the unconformity is not well-constrained, having been interpreted to represent a hiatus ranging from 10 m.y. in the west up to 34 m.y. in the east (Sando, 1988). Paleocaves and other paleokarst features such as pipes/sinkholes and collapse breccias that extend from the top of the unconformable surface well into the Formation characterize the top of the Upper Madison

Formation. These features are interpreted to have formed when the Madison platform was subaerially exposed.

North African Platform

Bechar Basin, Algeria

The Bechar Basin in northwestern Algeria (Madi et al., 2000; Cozar et al., 2014) was located between 10° - 15° S during the mid-Carboniferous (Scotese and McKerrow, 1990; Fig. 1) and was part of an elongate trough that extended from the eastern Morocco Anti-Atlas to Tunisia (Bourque et al., 1995). It is bounded to the north by the South Atlas fault, to the south by the Sbaa Basin, to the west by the Ougarta belt and to the east by the Talemzane arch (Bourque et al., 1995; Madi et al., 2000). This relatively deep basin contains some of the most continuous Carboniferous deposits on the Saharan Platform (Madi et al., 2000; Cozar et al., 2014). The Carboniferous succession here is dominated by open marine carbonates with some interbedded sandstones that lie unconformably on Devonian sandstones (Bourque et al., 1995; Atif and Legrand-Blain, 2011).

The stratigraphic record for this area is well constrained by conodont, foraminifera and ammonoid biostratigraphy (e.g. Manger et al., 1985; Wendt et al., 2009, 2010; Sommerville et al., 2013; Cozar et al., 2014). This robust age control allows for detailed correlation with other basins/regions.

The Mississippian (Serpukhovian) strata consist of limestones of the Djenien Formation and Lower Tangana Formation, while Lower Pennsylvanian (Bashkirian) is made up of limestones of the Lower to Upper Tangana Formation (Manger et al., 1985; Fig. 3). The Mississippian-Pennsylvanian boundary within the carbonate-dominated

sequence here lies within the Lower Tangana Formation and is not marked by an lithologic breaks but exhibits a general shallowing of facies across through the Lower Tangana Formation (Manger et al., 1985; Sabbar and Ouali, 1996; Fig. 3). The facies across the boundary interval changes from a bioclastic wackestone (Serpukhovian) to an oolitic grainstone with some intraclast (Bashkirian) deposited in a high-energy environment (Sabbar and Ouali, 1996). Conversely, biostratigraphic studies across the boundary suggest a hiatus of about 1 m.y. due to the absence of some conodont taxa (Saunders and Ramsbottom, 1986 and Sanz-Lopez et al., 2006).

Europe

Northwest Spain

La Lastra (Palentian Zone) in the Cantabrian Mountains, Northwest Spain was located between 5 – 15° S during the Carboniferous (Scotese and Mckerrow, 1990; Golonka and Ford, 2000). Carboniferous strata consist of the Genicera Formation limestone (Visean), the Alba Formation (Serpukhovian) the Barcaliente Formation limestones (Serpukhovian – Lower Bashkirian), which are disconformably overlain by the Perapertu Formation mudstones (Upper Bashkirian – Lower Moscovian).

Unlike most of the sections examined in this study, the Barcaliente Formation, which hosts rocks of Mississippian - Pennsylvanian age was deposited in a foredeep basin (Sanz-Lopez et al., 2006). The Barcaliente Formation is interpreted as distal turbidites made up dark bedded highly organic and typically shaly and laminated limestone (Gonzalez Lastra 1978; García-López, and Sanz-López, 2002).

Excellent chronostratigraphic control makes this section one of the best

constrained of mid-Carboniferous records, (Menendez-Alvarez, 1991; Sanz-Lopez et al., 2006,2013; Nemyrovska et al., 2008, 2011; Sanz-Lopez and Blanco-Ferrera 2013) and thus allows for detailed correlation with other regions.

The mid-Carboniferous boundary is placed in the Lower Barcaliente Formation (a black laminated limestone), about 2.5 to 2.8 m above the base of the formation (Sanz-Lopez et al., 2006) and is not marked by an unconformity (Hemleben and Reuther, 1980; Sanz-Lopez and Blanco-Ferrera 2013; Fig. 3) but rather exhibits a basinward shift in facies, interpreted to represent a shallowing trend to lagoonal intertidal to supratidal conditions (Sanz-Lopez et al., 2006, 2013). The gradual change in facies across the boundary is made up of laminated calcisiltites with silt-sized bioclastic grains and some bioturbation to peloidal wackestone with larger amounts of silt size materials and extensive bioturbation above the boundary (Sanz-Lopez et al., 2006, 2013). Additionally, this shallowing trend recorded through Serpukhovian to Lower Bashkirian strata of the Barcaliente is followed by relatively deep conditions marked by deposition of fine mud and peloids then back to shallow conditions at the top to ultimately cumulate in an erosional surface at the top of the Barcaliente Formation (Sanz-Lopez et al., 2006).

Central Taurides, Turkey

The central Taurides of Turkey were situated at 10 – 20° S during the Carboniferous (Golonka and Ford, 2000). The almost complete Upper Paleozoic succession is contained within the Aladag Unit in the Hardim Central Taurides, where Carboniferous strata consist of open marine shallow water carbonates with intercalated quartz arenites (Yilmaz and Altiner, 2006; Atakul-Ozdemir et al., 2011). The Yaricak

Formation of the Carboniferous is made up of two members, a Lower Member; Cityayka Member (Tournaisian) composed of thinly bedded limestones, siltstones and shale, and an Upper Member Mantar Tepe (Latest Tournaisian to Gzhelian) composed of limestones and arenitic sandstones (Atakul-Ozdemir et al., 2011; Fig. 3).

Both conodont and foraminifera biostratigraphic studies in the Central Tauridies of Turkey have allowed for a well-constrained chronostratigraphic framework and allowed for easy correlation with other regions around the globe (Atakul-Ozdemir et al., 2011, 2012). The mid-Carboniferous boundary interval here is not associated with a major unconformity or sequence boundary, but instead records a gradual shallowing of facies in the Mantar Tepe Member of the Yaricak Formation (Fig. 3). Serpukhovian strata below the boundary consists of bioclastic grainstone deposited below fair-weather wave base and Lower Bashkirian strata consist of oolitic and intraclastic grainstone deposited in wave agitated conditions (Atakul-Ozdemir et al., 2011).

The carbonate dominated Yaricak Formation, which spans the entire interval here is also dominated by high frequency cyclic deposits, arranged in a shallowing upward succession that appears to record gradual lowering of sea level during the Serpukhovian - Bashkirian interval (Atakul-Ozdemir et al., 2011).

Donets Basin (Ukraine)

The Donets Basin of Eastern Ukraine was situated between 10 – 15° N in a tropical to subtropical environment that occupied most of Eastern Europe (Scotese and McKerrow, 1990; Golonka and Ford, 2000). It is part of the Dnieper-Donets intracratonic rift basin with a northwest – southeast orientation (Eros et al, 2012; Ogar, 2012). The

stratigraphic nomenclature within the Donets Basin utilizes a set of upper case letters, A through S to designate Formations based on biostratigraphic constraints of marine limestones (Menning et al., 2006; Eros et al., 2012). As a result the chronostratigraphic framework of the area is very well constrained. In the Donets ramp, the Paleozoic strata are divided into three groups; Early Carboniferous (Tournaisian to Latest Visean) predominantly composed of shallow shelf limestones, grouped into the Mokorovolnovakha Series (Davydov et al., 2010; Ogar, 2012). The middle interval (Serpukhovian to Gzhelian) is composed of terrigenous clastics with intercalated beds of limestone (Skipp et al., 1989; Menning et al., 2006; Davydov et al., 2010; Ogar, 2012). This succession is divided into fifteen formations; each beginning with a marine limestone designated by an upper case letter with a superscript and subscript numeral (Davydov et al., 2010). Finally an upper (Gzhelian - Asselian) succession composed entirely of siliciclastics (Davydov et al., 2010; Ogar, 2012).

The well-constrained chronostratigraphic framework makes use of conodonts and high precision U-Pb absolute age yields from volcanic ash layers interbedded in the succession (Aizenverg et al., 1983; Davydov et al., 2010; Ogar, 2012), this has allowed for detailed correlation with other regions. Ammonoids and fusulinids are also extremely useful in the age control within this region (Davydov et al., 2010).

The Mississippian - Pennsylvanian boundary interval is placed at the base of limestone D^{5}_{8}upper and not associated with any unconformity or erosional surface (Skipp et al., 1989; Nemyrovska, 1999; Davydov et al., 2010; Fig. 3). However, across the boundary interval is a change from limestone into fluvial sandstone, which has been attributed to represent a sea level lowstand (Ogar, 2012; Eros et al., 2012). This lowstand

recognized in the Donets succession has been interpreted to correspond broadly with the timing of glacial maximum inferred from the distribution of glacigenic deposits in high-latitude Gondwana basins (Eros et al., 2012).

South Ural Mountains Russia

During the Carboniferous, the southern Urals were situated between 15 – 25° N and were part of the tropical to subtropical environment that occupied almost all of eastern Europe (Golonka and Ford, 2000). The region was dominated by shallow – marine carbonate, and siliceous-carbonates (Menning et al., 2006; Kulagina et al., 2013) whose growth was enhanced by the uplift of the Ural Mountains.

Excellent conodont, ammonoids and foraminifera biostratigraphic records of sections from this region makes the Mississippian-Pennsylvanian interval within this region well constrained (Brand and Bruckschen, 2002; Kalangina et al., 2013). This robust age control allows for detailed correlation to be made with other regions. Additionally, this region contains one of the most complete stratigraphic records through the Mississippian-Pennsylvanian interval. The Russian system uses sets of horizon and or Formations names to delineate lithostratigraphic units.

Two sections of the South Urals region were looked at in this study, the Muradymovo section which contains the most complete and continuous Carboniferous strata is part of the South Western Uralian megazone, west of the Zilair Megasynclinorium (Kulagina et al., 2013) and the Askyn River section located west of the Asatau anticline (Brand and Bruckschen, 2002). Serpukhovian to Bashkirian strata of the Muradymovo section are contained within the Bukharcha Formation, which is

composed of limestones with spongolite, argillite, argillaceous chert shale and nodular chert interbeds (Kulagina et al., 2013). While Serpukhovian to Bashkirian strata of the Askyn River section are made up of limestones and dolostones deposited in an open marine to semi-restricted shallow environment (Sinitsyna et al., 1995; Brand and Bruckschen, 2002). In the Askyn River section, horizons instead of formations names are used to designate lithologic breaks, thus late Serpukhovian strata are made up of the Brazhkian horizon, while Bashkirian strata from bottom to top comprise Bogdanovkian, Syuranian, Akavasian, Askynbashian, Tashastian, Asatauian and Solonstian horizons (Groves et al., 1999; Brand and Bruckschen, 2002).

In the Muradymovo section, the Mississippian – Pennsylvanian boundary interval is placed within the lower carbonate dominated successions of the Bukharcha Formation and is not associated with an unconformity (Proust et al., 1998; Kulagina et al., 2013; Fig. 3). Even though the boundary interval is not marked by an unconformity, a facies change is seen across the boundary, from thinly bedded limestone to bioclastic mudstone and wackestone with lithoclastic packstone that grades into limestone breccia (Kulagina et al., 2013). As with the NW Spain and Donets regions, the succession has been interpreted as recording a gradual sea level drop through the Mississippian – Pennsylvanian boundary interval. However, in the Askyn River section, an erosional unconformity representing about 1 m.y. hiatus is reported across the Mississippian – Pennsylvanian boundary interval (Groves et al., 1999). This hiatus at the Mississippian - Pennsylvanian boundary interval was further illustrated by isotopic data of Brand and Bruckschen (2002) from other measured sections within the Askyn River region.

South China

The South China platform was location between 0 – 15 S of the paleoequator in the Paleo-Tethys Ocean (Scotese and McKerrow, 1990; Golanka and Ford, 2000). During the Carboniferous Southern China was a broad flat terrain composed of two provinces and various sub basins formed in an extensional tectonic regime, the two provinces were; the Yangtze and the Southeast province (Wang et al., 2013). This configuration allowed for widespread deposition of relatively continuous shallow water carbonate sequences rich in marine fossils (Wang et al., 2013). Mississippian - Pennsylvanian strata in the region consist of Laobandong Formation, a dolostone that is disconformably overlain by grainstone – packstone limestones of the Huanglong Formation deposited in an open marine setting (Zhi, 1985; Wang et al., 2013).

Excellent chronostratigraphic control on the successions in South China are made possible through conodont, foraminifer, ammonoid and fusulinid biostratigraphy (Jing-Zhi, 1985; Zhihao et al., 1987; Zhihao and Yuping, 2003). These have allowed for understanding of the Mississippian - Pennsylvanian strata and provided a useful means for correlation of the boundary interval with other regions of Europe and North America. Additionally, the South China platform provides the ideal setting for study of eustatic fluctuations, because of the relative tectonic stability of the platform during the Carboniferous (Wang et al., 2013).

The Mississippian – Pennsylvanian interval in South China is marked in many areas by a disconformity and a facies change from tidal flat dolostones to pure limestones (Zhi, 1985, Zhihao et al., 1987; Wang et al., 2013; Fig. 3). This change in facies has been attributed to a major drop in sea level that can be traced throughout the region (Wang et

al., 2013). However, in some parts of the Lower Yangtze Mississippian – Pennsylvanian strata of carbonate dominance are marked by an erosional surface(Wang et al., 2013).

DISCUSSION

With the exception of Arrow Canyon, Algeria, Northwest Spain, Central Taurides, Turkey and Donets Basin (Ukraine), the interval that encompasses the mid-Carboniferous boundary is in many regions represented by a major exposure surface, erosional unconformity or disconformity surface (Fig. 3). While the above sites are not all associated with a major unconformity, a basinward shift in facies is recorded within most of the sections. In places where present, the duration of the unconformity has been estimated to range from 1 – 34 m.y.

For the Arrow Canyon section, Richard et al. (2001), Barnett and Wright (2008) and Bishop et al. (2009) interpreted the facies shift across the boundary interval, coupled with the exposure surfaces that occur above the boundary to record a drop in sea level. In the United States Midcontinent, the formation of an erosional unconformity across the Mississippian – Pennsylvanian boundary interval, coupled with the overall shallowing of facies capped by paleosol and paleokarst surfaces are interpreted to be consistent with a drop in sea level (Manger and Sutherland, 1992; Webb, 1994). This regression was followed by subsequent transgression in the Morrowan that led to the deposition of rocky shore deposits with siltstone, sandstone and shale (Manger and Sutherland, 1992; Webb, 1994). For the Spanish section in the Cantabrian Mountains, which was deposited in a deep marine setting, a gradual shallowing of facies that terminates at an erosional surface at the top of the Bracaliente Formation (Upper Bashkirian) (Nemyrovska et al., 2011) is

recorded across the successions. This change in facies has been attributed to gradual lowering of relative sea level (Nemyrovska et al., 2011). Additionally, the Donets and Turkey succession, which show similar patterns, records no major unconformity at the Mississippian – Pennsylvanian boundary interval, but the gradual shallowing of facies (Atakul-Ozdemier et al, 2012; Eros et al., 2012) across the interval has been interpreted to have resulted from gradual lowering of sea level (Atakul-Ozdemir et al., 2011; Eros et al., 2012). However, Central Taurides, Turkey at the time was undergoing tectonic subsidence (Stepphenson et al., 2006), and thus the lack of an unconformity in the basin may be attributed to the fact that rate of subsidence most likely outpaced the eustatic fall.

With such widespread similarity in stratigraphic successions, and the global synchroneity in a basinward shift of facies and or subaerial exposure surface recorded across the Mississippian – Pennsylvanian boundary intervals, interpreted to have resulted from drop in sea level. Therefore, suggesting the widespread unconformity that encompasses the Mississippian – Pennsylvanian boundary was formed most likely from a eustatic effect; i.e. lowering of global sea level. The lowering of relative sea level recorded at successions in Arrow Canyon, U.S. Midcontinent, Madison Platform, Big Horn Basin, WY, Bechar Basin, Algeria, Palentian Zone, Cantabrian Mountains, Northwest Spain, Central Taurides, Turkey, Donets Basin, Ukraine, Southern Ural Mountains, Russia and South China Platform are also consistent with ice Gondwana ice buildup during the Late Mississippian. In addition to the stratigraphic records, stable isotope studies across the mid-Carboniferous show an increase in $\delta^{13}C$, which would imply a decrease in atmospheric pCO2 and $\delta^{18}O$ consistent with an increase in ice volume (Mii et al., 1999, 2000; Frank et al., 2008). Together these positive shifts in $\delta^{13}C$

and $\delta^{18}O$ show a global pattern that is consistent with the protracted drawdown of sea level from ice buildup.

On the other hand, local sedimentation and tectonic activities cannot be ignored, for example, in the Appalachians region, which was tectonically active during the Late Paleozoic, the unconformity that encompasses the Mississippian – Pennsylvanian boundary postdates the interval (Beuthin, 1994; Ettensohn, 1994). As a result, Beaumont (1994) and Ettensohn (1980, 1994) tectonism as the cause of the unconformity encompassing the Mississippian – Pennsylvanian interval. They illustrated this by using a lithospheric flexural stratigraphic model to suggest that an unconformity is largely of tectonic origin if part or all of the stratigraphic response that initiated the unconformity is as a result of series of flexural events associated with an orogeny (Beaumont, 1994 and Ettensohn, 1980, 1994). However, using single locations, such as the Appalachian region, to make an assertion that the widespread unconformity evident at the Mississippian - Pennsylvanian boundary resulted from tectonism alone is contentious. This is because evidence for a drop in sea level is recorded even in the most tectonically stable area at the time, the South China platform (Wang et al., 2013); this area was unaffected by the formation of the supercontinent of Pangea.

Therefore, it can be concluded from evidence of global stratigraphic patterns recorded in the successions addressed within this study and the synchroneity of basinward shift in facies interpreted to have resulted from drop in sea level recorded at the various sites that the origin of the unconformity the encompasses the Mississippian – Pennsylvanian boundary most likely resulted from a eustatic fall at the Serpukhovian – Bashkirian boundary, along with the interplay of high frequency glacioeustatic variations

in sea level. But in places where tectonism (uplift or subsidence) was prevalent such as the Appalachians etc. the effects of the eustatic drop were masked and tectonism may have played a bigger role in the stratigraphic patterns recorded in those areas.

CONCLUSIONS

A study of the Mississippian – Pennsylvanian carbonate successions which encompasses the Mississippian – Pennsylvanian boundary from cratonic settings of nine regions irrespective of the tectonic activity acting within the basin record the occurrence of a sequence boundary or a basinward shift in facies. The expression of the unconformity that includes the Mississippian - Pennsylvanian boundary varies greatly, with the duration of the hiatus ranging from 1 – 34 m.y.

Results from this study show a global synchroneity in stratigraphic patterns and a basinward shift in facies across the boundary interval that have been interpreted to record a drop in sea level. Together, the synchroneity of drop in sea level at the nine locations looked at in this study suggest that the unconformity that encompasses the Mississippian – Pennsylvanian interval was a result of eustatic fall associated with pronounced expansion of growing ice sheets in Gondwana. However this global effect in areas such as the Appalachians and the Central Taurides, was enhanced and/or masked as a result of the greater degree of local tectonic effects acting within the basin.

ACKNOWLEDGMENTS

This research was supported by NSF Grant EAR-0645504 to T. Frank and GSA grant to L. Nana Yobo.

References

Aretz, M., 2011. Corals from the Carboniferous of the central Sahara (Algeria); the collection 'Marie Legrand-Blain'. Geodiversitas, 33(4; 4), pp. 581-624.

Atakul-Ozdemir, A., Altiner, D., Ozkan-Altiner, S., and Yilzmaz, I. O., 2011. Foraminiferal biostratigraphy and sequence stratigraphy across the mid-Carboniferous boundary in the Central Taurides, Turkey: Facies, v 57, p. 705-730.

Atakul-Ozdemir, A., Altiner, D. and Ozkan-Altiner, S., 2012. Conodont distribution across the Mid-Carboniferous boundary in the central Taurides, Turkey. Rivista Italiana di Paleontologia e Stratigrafia, 118(2), pp. 213; 213-222.

Barnett, A.J., and Wright, V.P., 2008. A sedimentological and cyclostratigraphic evaluation of the completeness of the Mississippian-Pennsylvanian (Mid-Carboniferous) Global Stratotype Section and Point, Arrow Canyon, Nevada, USA: Geological Society of London Journal, v. 165, p. 859–873.

Beuthin, J.D., 1994, A sub-Pennsylvanian paleovalley system in the central Appalachian basin and its implications for tectonic and eustatic controls on the origin of the regional Mississippian–Pennsylvanian unconformity, SEPM Concepts in Sedimentology and Paleontology, v. 4, p. 107–120.

Bishop, W. F., 1975. Geology of Tunisia and adjacent parts of Algeria and Libya: AAPG Bull. v. 59, p413-450.

Bishop, W.J., Montanez, I.P., Gulbranson, E.L., and Brenckle, P.L., 2009: The Onset of mid-Carboniferous glacio-eustasy: Sedimentologic and diagenetic constraints, Arrow Canyon, Nevada, Palaeogeogr. Palaeoclimatol. Palaeoecol. vol. 276, pp. 217–243.

Blake, B.M., Beuthin, J. D., 2008. Deciphering the mid-Carboniferous eustatic even in central Appalachian foreland basin, southern West Virginia, USA. GSA Special Paper, 441, pp. 343–354.

Blakey, R.C., 2008. Gondwana paleogeography from assembly to breakup—a 500 m.y. odyssey. GSA Special Paper, 441, pp. 1–28.

Brand, U., and Bruckschen, P., 2002. Correlation of the Askyn River section, Southern Urals, Russia, with the Mid-Carboniferous Boundary GSSP, Bird Spring Formation, Arrow Canyon, Nevada, USA: implications for global paleoceanography. Palaeogeography, Palaeoclimatology, Palaeoecology 184, 177-193

Brenckle, P.L., Baesemann, J.F., Lane, H.R., West, R.R., Webster, G.D., Langenheim, R.L., Brand, U. and Richards, B.C., 1997. Arrow Canyon, the Mid-Carboniferous boundary stratotype. Prace Panstwowego Instytutu Geologicznego [1988], 157, Part 3, pp. 149-164.

Bourque, P-A., A. Madi, and B. Mamet, 1995. Waulsortian-type bioherm development and response to sea level fluctuations: upper Visean of Bechar basin, western Algeria: JSR, v. B65, no. 1, p. 80–95.

Cózar, P., Vachard, D., Somerville, I.D., Medina-Varea, P., Rodríguez, S. and Said, I., 2014. The Tindouf Basin, a marine refuge during the Serpukhovian (Carboniferous) mass extinction in the northwestern Gondwana platform. Palaeogeography, Palaeoclimatology, Palaeoecology, 394(0), pp. 12-28.

Davydov, V.I., Crowley, J.L., Schmitz, M.D. and Poletaev, V.I., 2010. High-precision U-Pb zircon age calibration of the global Carboniferous time scale and Milankovitch band cyclicity in the Donets Basin, eastern Ukraine. Geochemistry, Geophysics, Geosystems - G [super 3], 11(2; 2), pp. @CitationQ0AA04-@CitationQ0AA04.

Eros, J.M., Montanez, I.P., Davydov, V.I., Osleger, D.A., Nemyrovska, T.I., Poletaev, V.I. and Zhykalyak, M.V., 2012. Sequence stratigraphy and onlap history of the Donets Basin, Ukraine; insight into Carboniferous icehouse dynamics; reply. Palaeogeography, Palaeoclimatology, Palaeoecology, 363-364, pp. 187-191.

Ettenshohn, F.R., 1980. An alternate to the barrier-shorline model for deposition of the Mississippian and Pennsylvanian rocks in northeastern Kentucky: summary. GSA Bulletin v91, p. 130-135.

Fielding, C.R., Frank, T.D., Birgenheier, L.P., Rygel, M.C., Jones, A.T., Roberts, J., 2008a. Alternating glacial and non-glacial intervals characterize the late Paleozoic Ice Age: stratigraphic evidence from eastern Australia. Journal of the Geological Society of London 165, 129–140.

Fielding, C.R., Frank, T.D., Isbell, J.L., 2008b. The late Paleozoic ice age—a review of current understanding and synthesis of global climate patterns. In: Fielding, C.R., Frank, T.D., Isbell, J.L. (Eds.), Resolving the Late Paleozoic Ice Age in Time and Space: Geological Society of America Special Paper, 441, pp. 343–354.

Fielding, C.R., Frank, T.D., Isbell, J.L. (Eds.), 2008c. Resolving the Late Paleozoic Ice Age inTime and Space: Geological Society of America Special Paper, 441. 354 pp.

Frank, T.D., Birgenheier, L.P., Montañez, I.P., Fielding, C.R., Rygel, M.C., 2008. Controls on late Paleozoic climate revealed by comparison of near-field stratigraphic and farfield stable isotopic records. GSA Special Paper, 441, pp. 331–342.

García-López, S. & Sanz-López, J. 2002. Devonian to Lower Carboniferous conodont biostratigraphy of the Bernesga Valley section (Cantabrian Zone, NW Spain). In: García-López, S. & Bastida, F. (eds.), Palaeozoic Conodonts from Northern Spain. Cuadernos del Museo Geominero, 1: 163-205.

Gradstein, F.M., Ogg, J.G., Schmitz, M.D., and OGG, G.M., (Eds.), 2012. A Geologic Time Scale 2012. Elsevier: Oxford, United Kingdom.

Golonka, J., Ford, D., 2000. Pangean (Late Carboniferous–Middle Jurassic) palaeoenvironment and lithofacies. Palaeogeography Palaeoclimatology Palaeoecology 161, 1–34.

Goldhammer R.K., Dunn P.A., Hardie L.A., 1990. Depositional cycles, composite sea-level changes, cycle stacking patterns, and their hierarchy of stratigraphic forcing: examples from Alpine Triassic platform carbonates. Geol Soc Am Bull 102:535–562

González Lastra, J., 1978. Facies salinas en la Caliza de Montaña (Cordillera Cantábrica). Trabajos de Geología, Universidad de Oviedo, 10: 249-265.

Groves J. R., Nemyrovska T. I. & Alekseev A. S. 1999. Correlation of the type Bashkirian Stage (MiddÌe Carboniferous, South Urals) with the Morrowan and Atokan Series of the Midcontinentl and western United States. Journal of Paleontology 73(3): 529 -539

Hemleben, C., and Reuther, C., 1980. Allodapic limestones of the Barcaliente Formation (Namurian A) between Luna and Cea rivers (southern Cantabrian Mountains, Spain). Neues Jahrbuch fuer Geologie und Palaeontologie.Abhandlungen, 159(2; 2), pp. 225-255.

Higgins, A.C., 1981. The position and correlation of the boundary between the proposed Mississippian/Pennsylvanian subsystems. Newsletters on Stratigraphy, 9(3), pp. 176; 176-182.

Isbell, J.L., Lenaker, P.A., Askin, R.A., Miller, M.F., Babcock, L.E., 2003. Reevaluation of the timing and extent of late Paleozoic glaciation in Gondwana: Role of the Transantarctic Mountains Geology, November, 2003, v. 31, p. 977-980.

Kulagina, E., Nikolaeva, S., Pazukhin, V. and Kochetova, N., 2014. Biostratigraphy and lithostratigraphy of the Mid-Carboniferous boundary beds in the Muradymovo section (South Urals, Russia). Geological Magazine, 151(2), pp. 269-298.

Lane, H.R., Brenckle, P.L., Baesemann, J.F., and Richards, B.F., 1999, The IUGS boundary in the middle of the Carboniferous: Arrow Canyon, Nevada USA: Episodes, v. 22, p. 272–283.

Lemosquet, Y., Pareyn, C., 1985. North Africa, Bechar Basin. In: Wagner, R.H., Winkler Prins, C.F., Granados, L.F. (Eds.), The Carboniferous of the world, 2, Australia, Indian subcontinent, South Africa, South America & North Africa, IUGS Publication 20, pp. 306–315.

Madi, A, Savard, M. M.,Bourque P-A, and Chi. G., 2000. Hydrocarbon potential of the Mississippian carbonate platform, Bechar Basin, Algerian Sahara AAPG Bull. v. 84(2) p. 266-287.

Manger, W.L., Weyant, M., Pareyn, C., 1985. Mid-carboniferous ammonoid stratigraphy, Bechar Basin, Algeria. Cour. Forsch. Inst. Senckenberg 74,181–196.

Menning, M., Alekseev, A. S., Chuvashov, B.I., Davydov, V.I., Devuyst, F.-X., Forke, H.C., Grunt, T.A., Hance, L., Heckel, P.N., Izokh, N.G., Jin, Y.-G., Jones, P.J., Kotlyar, G.V., Kozur, H.W., Nemyrovska, T.I., Schneider, J.W., Wang, X.-D., Weddige, K., Weyer, D. & Work, D.M., 2006. Global time scale and regional stratigraphic reference scales of Central and West Europe, Tethys, South China and North America as used in the Devonian-Carboniferous-Permian Correlation Chart (DCP 2003). Palaeogeography, Palaeoclimatology, Palaeoecology, 240, 318-372.

Mii, H., Grossman, E.L., and Yancey, T.E., (1999) Carboniferous isotope stratigraphies of North America: Implications for Carboniferous paleoceanography and Mississippian glaciation. GSA Bulletin 111, 960-973.

Miller, D. J., and K. A. Eriksson, 1997, Late Mississippian prodeltaic rhythmites in the Appalachian basin: a hierarchical record of and climatic periodicities: Journal of Sedimentary Research, v. 67, p. 653–660.

Nemirovskaya, T.I., Poletaev, V.I. and Vdovenko, M.V., 1990. The Kal'mius section, Donbass, Ukraine, U.S.S.R.; a Soviet proposal for the Mid-Carboniferous boundary stratotype. CFS.Courier Forschungsinstitut Senckenberg, 130, pp. 247-272.

Nemyrovska, T.I., Wagner, R.H., Winkler Prins, C.F. and Montanez, I., 2011. Conodont faunas across the Mid-Carboniferous boundary from the Barcaliente Formation at La Lastra (Palentian Zone, Cantabrian Mountains, northwest Spain); geological setting, sedimentological characters and faunal descriptions. Scripta Geologica, 143, pp. 127-183.

Osipova, A.I. and Belskaya, T.N., 1987. Mid-Carboniferous boundary on the Russian Platform and on the western slope of the Urals. Compte Rendu - Congres International de Stratigraphie et de Geologie du Carbonifere = International Congress on Carboniferous Stratigraphy and Geology., 11, pp. 361-361.

Pareyn, C., Saunders, W.B., Manger, W.L. And Lemosquet, Y., 1984. Compte Rendu - Congres International de Stratigraphie et de Geologie du Carbonifere = International Congress on Carboniferous Stratigraphy and Geology.

Pareyn, C., 1961. Les Massifs Carbonifères du Sahara Sud-Oranais. Publications du Centre de Recherches sahariennes, Série Géologie,1: 1-324.

Pique, A., Bossiere, G., Bouillin, J., Chalouan, A. And Hoepffner, C., 1993. Southern margin of the Variscan Belt; the north-western Gondwana mobile zone (eastern Morocco and northern Algeria). Geologische Rundschau, 82(3; 3), pp. 432-439.

Pierce, R.W., Langenheim Jr., R.L., 1972. Platform condonts of the Monte Cristo Group, Mississippian, Arrow Canyon Range, Clark Country, Nevada. J. Paleontol. 48, 149–169.

Poole, F.G., Sandberg, C.A., 1991. Mississippian paleogeography and conodont biostratigraphy of the western United Stat. In: Cooper, J.D., Stevens, C.H. (Eds.), Paleozoic Paleogeography of the Western United States—II. Pacific Section SEPM, vol. 67, pp. 107–136.

Proust, J.N., Chuvashov, B.I., Vennin, E. And Boisseau, T., 1998. Carbonate platform drowning in a foreland setting; the Mid-Carboniferous platform in western Urals (Russia). Journal of Sedimentary Research, 68(6), pp. 1175-1188.

Riley, N.J., Claoue-Long, J., Higgins, A.C., Owens, B., Spears, A., Taylor, L. and Varker, W.J., 1994. Geochronometry and geochemistry of the European Mid-Carboniferous boundary global stratotype proposal, Stonehead Beck, North Yorkshire, UK. Annales de la Societe Geologique de Belgique, 116(2), pp. 275; 275-289.

Ross, C.A. and Ross, J.R.P., 1985. Carboniferous and Early Permian biogeography. Geology, v. 13, pp. 27-30.

Rygel, M.C., Fielding, C.R., Frank, T.D., Birgenheier, L.P., 2008. The magnitude of late Paleozoic glacioeustatic fluctuations: a synthesis. Journal of Sedimentary Research, 78, 500–511.

Sebbar, A., and Ouali, R. A., 1996. Dynamique de la plate-forme carbonatee du Carbonifere du bassin de 'Bechar-Mezarif'; paleoenvironnements, bioconstructions. Bulletin - Office National de la Geologie, 7(2), pp. 229; 229-251.

Sando, W. J., 1988. Madison Limestone (Mississippian) paleokarst: a geologic synthesis. In: James, N.P., Choquette, P.W. (Eds.), Paleokarst. New York, Springer-Verlag, pp. 256-277.

Saunders, W. B., and W. H. C. Ramsbottom, 1986, The mid- Carboniferous eustatic event: Geology, v. 14, p. 208–212.

Sanz-López, J., Blanco-Ferrera, S., Sánchez de Posada, L.C. & García-López, S. 2006. The mid-Carboniferous boundary in northern Spain: difficulties for correlation of the global stratotype section and point. Rivista Italiana di Paleontologia e Stratigrafia, 112: 3-22.

Sanz-Lopez, J. and Blanco-Ferrera, S., 2013. Early evolution of Declinognathodus close to the Mid-Carboniferous boundary interval in the Barcaliente type section (Spain). Palaeontology, 56(5; 5), pp. 927-946.

Scotese, C.R., Langford, R.P., 1995. Pangea and the paleogeography of the Permian. In: Scholle, P.A., Peryt, T.M., Ulmer-Scholle, D.S. (Eds.), The Permian of Northern Pangea, volume 1. Springer-Verlag, New York, pp. 3–19.

Sinitsyna, Z.A., Kulagina, E.I., Pazukhin, V.N., Kochetkova, N.M., 1995. 5. Askyn section.

In: Kozlov, V.I., Sinitsyna, Z.A., Kulagina, E.I., Pazukhin, V.N., Puchkov, V.N., Kochetkova, N.M., Abramova, A.N., Klimenko, T.V., Sergeeva, N.D. (Eds.), Guidebook of Excursion for the Paleozoic and Upper Precambrian Sections of the Western Slope of the Southern Urals and Preuralian Regions. Geological Institute Ufa Science Center RASci., pp. 106-121.

Skipp, B.A., Brenckle, P.L., Poletaev, V.I., Nemirovskaya, T.I., Lane, H.R. and Manger, W.L., 1989. The continuing international search for a Mid-Carboniferous boundary stratotype; Donets Basin, USSR, 1988. Episodes, 12(3; 3), pp. 179-183.

Somerville, I.D., Cózar, P., Said, I., Vachard, D., Medina-Varea, P., Rodríguez, S., 2013. Palaeobiogeographic constraints on the distribution of foraminifers and rugose corals in the Carboniferous Tindouf Basin, S. Morocco. J. Palaeogeogr. 2, 1–18.

Sonnenfeld, M.D., 1996a. Sequence evolution and hierarchy within the lower Mississippian Madison Limestone of Wyoming, In: Longman, M.W., Sonnenfeld, M.D. (Eds.), Paleozoic Systems of the Rocky Mountain Region. Society for Economic Paleontologists and Mineralogists (Society for Sedimentary Geology) Rocky Mountain Section, pp. 165-192.

Tobin, K.J. and Driese, S.G., 2003. Echinoderm stabilization associated with a paleokarst surface at the Mississippian-Pennsylvanian boundary in Tennessee, U.S.A. Journal of Sedimentary Research, 73(2; 2), pp. 206-216.

Ueno, K., Hayakawa, N., Nakazawa, T., Wang, T. & Wang, X. 2012. Pennsylvanian–Early Permian cyclothemic succession on the Yangtze Carbonate Platform, South China. In: Ga˛siewicz, A. & Słowakiewicz, M. (eds) Palaeozoic Climate Cycles: Their Evolutionary and Sedimentological Impact. Geological Society, London, Special Publications, 376. First published online November 29, 2012,http://dx.doi.org/10.1144/SP376.5

Veevers, J.J., Powell, C. McA, 1987. Late Paleozoic glacial episodes in Gondwanaland reflected in transgressive–regressive depositional sequences in Euramerica. GSA Bulletin 98, 475–487.

Wang, X., Qie, W., Sheng, Q., Qi, Y., Wang, Y., Liao, Z., & Ueno, K. 2013. Carboniferous and Lower Permian sedimentological cycles and biotic events of South China. *Special Publication - Geological Society Of London*, *376*doi:10.1144/SP376.11

Wang Zhi-hao, Lane R. H., and Manger W. L., 1987 - Conodont sequence across the Mid-Carboniferous boundary in China and its correlation with England and North America. In: 'Wang Cheng-yuan (Ed.) – Carboniferous boundaries in China. pp. B9-106, Beijing.

Waters, C.N., and Condon, D.J., 2012. Nature and timing of Late Mississippian to Mid Pennsylvanian glacio-eustatic sea-level changes of the Pennine Basin, UK. Journal of the Geological Society 169, 37-51.

Wendt, J., Kaufmann. B., Belka, Z., and Korn, D., 2009. Carboniferous stratigraphy and depositional environments in the Ahnet Mouydir area (Algerian Sahara). Facies 55 (3): 443–472, DOI 10.1007/s10347-008-0176-y

Wilson, E.N., 1984. Nature of the Mississippian-Pennsylvanian unconformity in eastern Kentucky and vicinity. Compte Rendu - Congres International de Stratigraphie et de Geologie du Carbonifere = International Congress on Carboniferous Stratigraphy and Geology., 9 (2), pp. 345-356.

Woodard, S.C., Thomas, D.J., Grossman, E., Olszewski, T., Yancey, T., Raymond, A. and Miller, B.V., 2010. Nd isotopes as indicator of glacio-eustasy, Mid-Carboniferous boundary Arrow Canyon, NV. Geochimica et Cosmochimica Acta, 74(12; 12), pp. 1140-A1140.

Wright, V.P. & Vanstone, S.D. 2001. Onset of late Palaeozoic glacioeustasy and the evolving climates of low latitude areas: A synthesis of current understanding. Journal of the Geological Society, London, 158, 579–582.

Yılmaz, I.O., Altıner, D., 2006. Cyclic paleokarst surfaces in Aptian peritidal carbonate successions (Taurides, SW Turkey): internal structure and response to mid-Aptian sea-level fall. Cretaceous Res 27:814–827.

Zhi, Y. J.,1985. A preliminary discussion of the Mid-Carboniferous boundary in China. Compte Rendu - Congres International de Stratigraphie et de Geologie du Carbonifere = International Congress on Carboniferous Stratigraphy and Geology., 10, Vol. 4, pp. 341; 341-352.

CHAPTER TWO

OUTCROP CHARATERIZATION OF KARST DEVELOPMENT ON A SHALLOW ON CARBONATE PLATFORM: MISSISSIPPIAN MADISON FORMATION, BIGHORN BASIN, WYOMING, USA.

ABSTRACT

Although karsted carbonates are considered among the most attractive hydrocarbon reservoirs, their heterogeneous nature also makes them among the most complex. The karsted surface that caps the Mississippian Madison Formation is well-exposed in outcrops in the northeastern Bighorn Basin, WY, USA, providing an opportunity to examine development of key reservoir properties along a major karsted surface. Five closely spaced stratigraphic sections through extensive canyon exposures of the Mission Canyon Member (uppermost member of the Madison Formation) were studied to characterize lateral variation in karst development at the top of the unit. This member consists of a shallowing upward sequence developed in the restricted platform interior environment and consists of eight depositional facies. The unconformable surface is highly irregular and represents at least 10 million years of subaerial exposure and non-deposition. Karst features include large solution-enhanced fractures, vertical dissolution pipes, and cave systems. A laterally persistent stromatolite horizon, which occurs near the top of the Madison Formation, provides a datum against which the depth of karsting can be measured. Pipes and caves, which measure as much as 12 m wide and 20-30 m deep, often contain breccia consisting of cobble-to-boulder-sized limestone blocks with a red, fine-grained sandstone matrix. A second breccia type, characterized by a gray matrix breccia, occurs as a laterally continuous, stratabound horizon. The Darwin Sandstone

Member of the overlying Pennsylvanian Amsden Formation, a fine-grained, cross-bedded reddened quartzite, fills in the topography of the unconformable surface. This study provides an outcrop analog for understanding karsted reservoirs that will aid in the assessment of examples in the subsurface.

INTRODUCTION

The dissolution of carbonates from meteoric water during prolonged periods of subaerial exposure leads to the formation of karsted carbonates. These carbonate can lead to the formation of important hydrocarbon reservoirs, such as the Cerro-Azul-4 of the Golden Lane trend in Varacruz Mexico (Viniegra and Castillo-Tejero (1970), the Yates (Tinker and Mruk, 1995; Strafford et al., 2008) and Ellenburger (Loucks and Mescher, 1997) fields of West Texas, the Amposte oil field in offshore Mediterranean Spain (Seemen et al., 1990), the Nang oil field in the Gulf of Thailand (Heward et al., 2000), the Ordos Basin of China (Wang and Al-Aasm, 2002), the Tarim Basin of China (Boamin and Jongjiang, 2009) and the Elk Basin and Garland fields of the Mississippian Madison Formation in Wyoming, USA (Harris and Sieverdin, 1991 and Demiralin et al., 1993). The prolong subaerial exposure that often leads to the formation of these reservoirs also results in huge heterogeneity and reservoir complexities (Kerans, 1988) consequently understanding the scale and character of such reservoirs can be very difficult and pose huge complications for exploration geologist. Equally, the scarcity of data both in outcrop and subsurface sections makes it difficult to decipher and interpret these paleokarst

systems (Loucks, 1999 and Wright, 1991). Thus an understanding of how the karst features are formed is essential since the reconstruction of such processes are critical for exploration geologist to decipher when evaluating a reservoir. For this reason, a well-exposed outcrop (such as in the Bighorn Basin) provides good analog for understanding these karsted carbonates as well as some of the spatial complexities they possess.

In the Bighorn Basin of northern Wyoming, a major karsted horizon is exposed in outcrop over a broad region. The preserved paleokarst system formed as a result of the subaerial exposure of Madison Formation. Influx of meteoric water on the subaerially exposed surface led to the dissolution of evaporite beds and limestone layers. The deposition of the Darwin Sandstone Member of the Amsden Formation, a fine-grained, cross-bedded reddened quartzite, terminated the Madison hiatus, proposed to last up to about 34 m.y. within the region (Sando, 1988).

Previous studies within the Bighorn Basin have documented the presence of the evaporite karst system and the various characteristics of the breccia formed but none have incorporated isotopic analysis combined with observed sedimentologic characteristics to understanding the evolution of the Madison karst. Incorporating such data with observed sedimentologic characteristics are significant for exploration purposes since the reconstruction and classification of the heterogeneity of karst reservoirs are significant for exploration. Thus, the purpose of this study is to examine the regional expression of this karsted interval that lies atop the Madison Formation and marks the Mississippian – Pennsylvanian boundary, through the observed sedimentology and stratigraphy as well petrographic thin section and stable isotope data, and to understand the regional expression of the karsted interval and its spatial complexity as an analog for assessment

of examples in the subsurface. These findings will aid in assessment of future hydrocarbon exploration efforts within this region and elsewhere.

GEOLOGIC SETTING

LOCATION:

This study focuses on outcrops in the Bighorn Basin, which is located in northeastern Wyoming, USA (Fig. 1). It is bordered to the south by the Owl Creek Mountains, and to the north by the Lewis and Clark lineament. The Bighorn Mountains lie to the east and Absaroka volcanics to the west (Blackstone and Huntoon, 1984; Katz et al., 2006). This area was chosen for the study because of the karsted surface that caps the Madison Formation is exposed over a broad region and easily accessible.

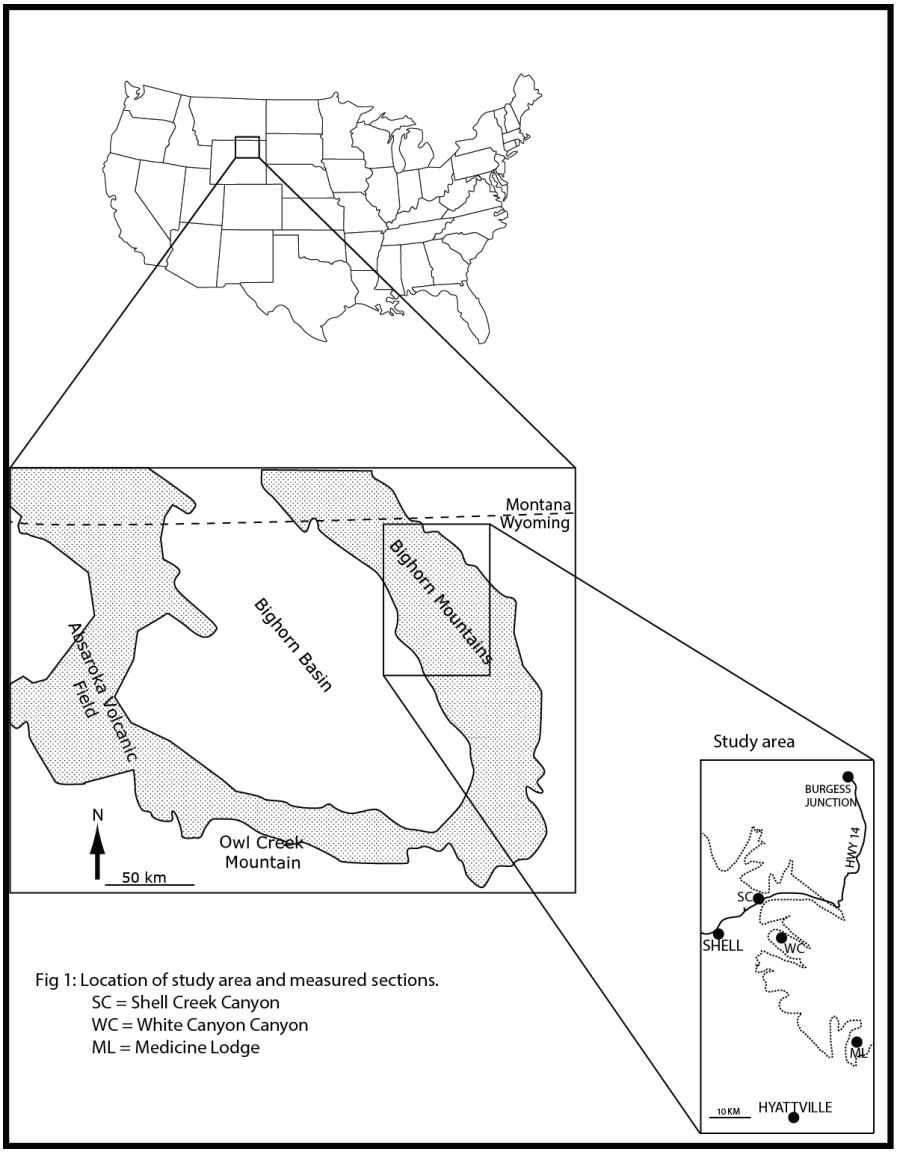

Fig 1: Location of study area and measured sections.
SC = Shell Creek Canyon
WC = White Canyon Canyon
ML = Medicine Lodge

Fig: 1. Map showing location of study area and measured sections within Bighorn Basin.

PALEOGEOGRAPHY

Carbonates of the Madison Formation accumulated on a broad epeiric platform known as the Madison Platform (Gutshick and Sandberg, 1983), which was active from Kinderhookian to Early Meramecian time (Sando, 1988). This platform was dominated by shallow marine environments, was located at about 5˚ N of the paleoequator (McKerrow and Scotese, 1990), and extended for 1600 km from Canada south into New Mexico and Arizona, USA (Sando, 1988). The platform was bound to the north by the central Montana trough and the Williston Basin, to the south and southeast by the Leadville and Redwell shelf and the transcontinental arch while the Antler highland and foreland basin bounds it to the west (Fig. 2) (Gutshick and Sandberg, 1983; Sonnenfield, 1996a).

The Antler and associated forelands development to the to the west that began in the Late Devonian resulted in increased subsidence and created the accommodation space for carbonate deposition (Gutshick and Sandberg, 1983; Sando, 1988; Sonnenfield, 1996a). The effects of this orogenesis extended well into the Middle to Late Mississippian, as evidenced by syn-orogenic sedimentation and erosion in Middle Mississippian strata in Nevada and Utah (Trexler et al., 2003). The deposition of the Madison Formation was finally terminated by a regional subaerial unconformity characterized by an extensive paleokarst (Sando, 1998).

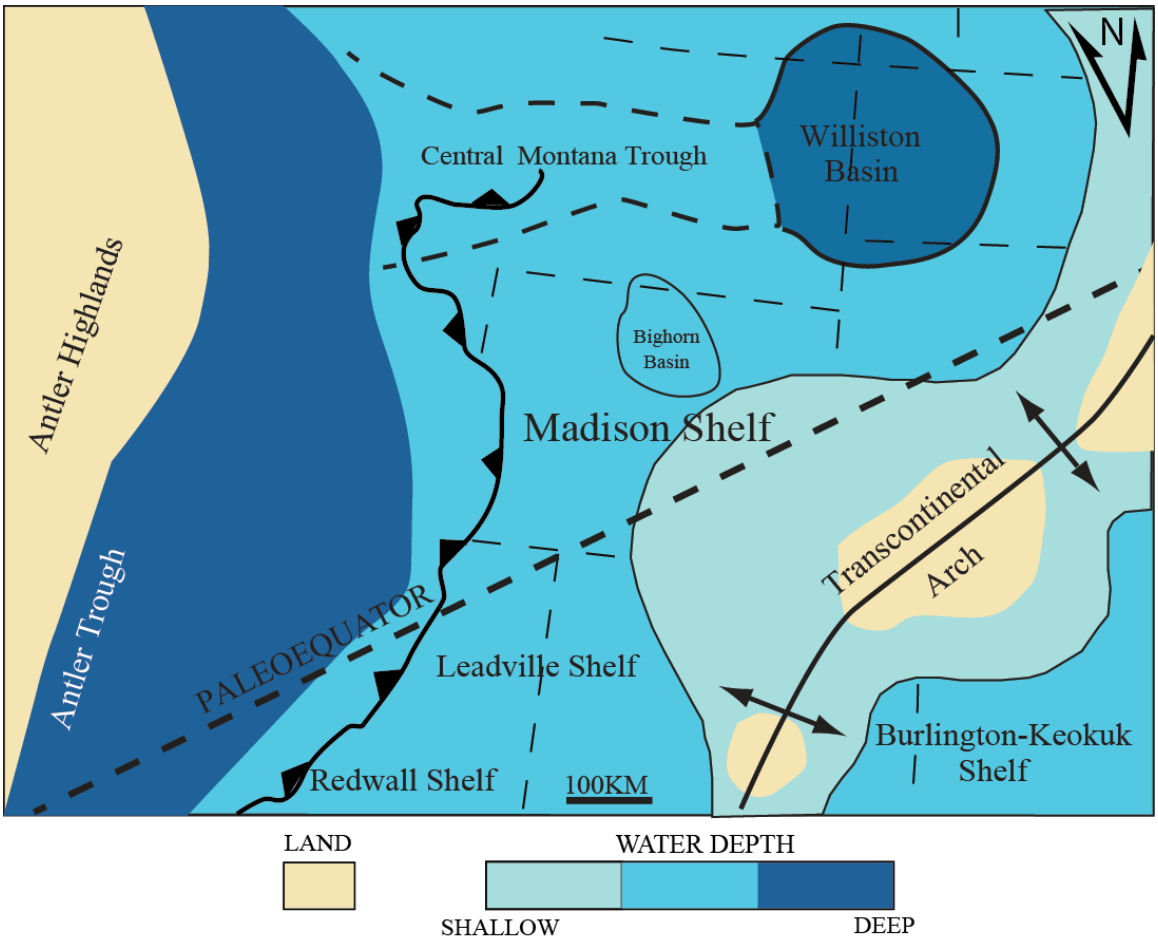

Fig 2: Regional paleogeography map of the Madison Platform modified after Gutschick and Sandberg (1983) and Sonnenfeld (1996). Illustrated in this map also are the tectonic configuration present during that time and an outline of where the Bighorn Basin would have been situated. Also shown is the generalized location of the post Mississippian Sevier thrust.

STRATIGRAPHIC FRAMEWORK

The Madison Formation is a 2nd order supersequence that was deposited on a shallow marine platform (Vail et al., 1977; Sando, 1998). It is divided into two members, a lower member, the Lodgepole Limestone and an upper member, the Mission Canyon Limestone (Collier and Cather 1922; Fig. 3). Several stratigraphic nomenclatures exist for the Madison, but for the purpose of this study the stratigraphic hierarchies and terminologies of the Madison as defined by Sonnenfeld (1996a, b) are used. The Madison is made up of two composite sequences and six 3rd order sequences. The 3rd order sequences represent about 2 m.y. years each for a total time of about 12 m.y. years represented (Sando, 1985; Sonnefeld, 1996a, b; Smith et al., 2004).

Sequences I – III lie within the Lodgepole Limestone, while sequences IV through VI lie within the Mission Canyon Limestone. Sequences III through VI, deposited between Early Osagean and Meramecian time, record the maximum inundation in the Wyoming shelf and contain two laterally extensive solution breccias interpreted to represent exposure of the platform (Sando, 1985, 1988; Elrick, 1990; Vice and Utgaard, 1989; Sonnenfeld, 1996 and Buoniconti, 2008).

Termination of the Madison is marked by a regionally extensive unconformity that mat lasted up to 34 m.y. in the east of the basin as a result of widespread platform exposure (Sando, 1988; Sonnenfeld 1996). This prolonged period of exposure allowed for karstification of the Madison and resulted in variable erosion of the upper Madison Formation (Sando, 1988). Isopach of the Madison by Andrichuk (1955) illustrates a north and west thickening parallel to progradation in the Central Montana Trough and the

Antler Trough.

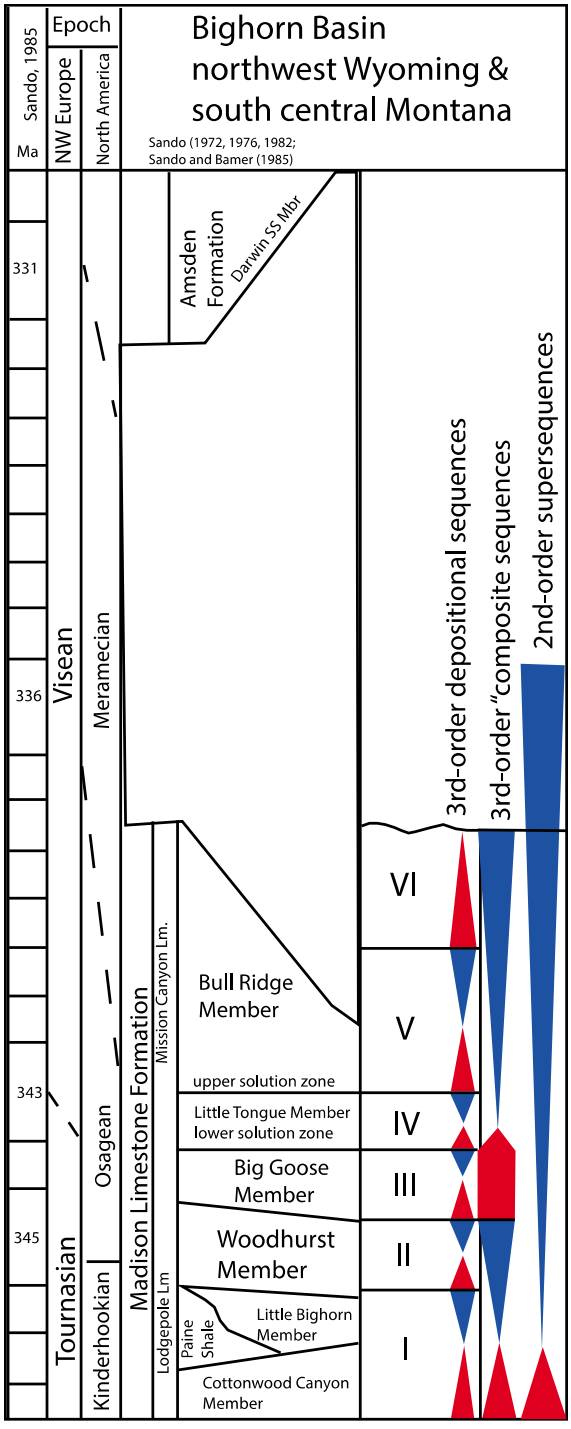

Fig. 3: Chronostratigraphic chart showing the lithostratigraphic units in the Bighorn Basin of northern Wyoming and time gap within the Madison Formation. Blue triangles represent increase in accommodation and red triangles represents decreased. Modified

from Sonnenfeld (1996b).

METHODS

Fieldwork was carriedout in northeastern Bighorn Basin, Wyoming where the Madison Formation often occurs in sheer cliff face exposures, making it difficult to access. The most accessible exposures occur in extensive canyons that provide cuts through the formation. Five closely spaced stratigraphic sections through the Mission Canyon Member (uppermost member of the Madison Formation) were measured along Shell Creek Canyon, White Creek Canyon, and in Medicine Lodge Park (Fig. 1). Sedimentological data including fossil types, sedimentary structures, grain size, bed thickness, lateral and vertical bedding trends, and nature of contacts were collected and used in the interpretation of facies and depositional environment. Samples were also collected for petrographic and isotopic analysis.

Samples collected from outcrop were thin sectioned and analyzed using standard petrographic and cathodoluminescence microscopy to document sediment textures, grain types, and diagenetic features. This information in addition to outcrop observations was used for understanding of the depositional environment and facies trends across the interval.

Using a microscope-mounted microdrill assembly with dental bits of 500 microns in diameter, 86 samples (100 to 200 micrograms) of matrix micrite were collected to generate a carbon isotope curve to facilitate correlation. Isotopic analyses were carried out at Keck Paleoenvironmental and Environmental Stable Isotope Laboratory (KPESIL) at the University of Kansas using a ThermoFinnigan GasBench II in-line with a Finnigan

MAT 253 isotope ratio mass spectrometer. Results are reported in permil relative to the Vienna Pee Dee Belemnite (VPDB) isotope standard. Precision was better than 0.06‰ for d13C and 0.12‰ for d18O values, determined through comparison with National Bureau of standards (NBS) 18 Carbonatite [National Institute of Standards and Technology (NIST) reference material # 8543] and NBS 19 Limestone (NIST reference material # 8544), and NIST reference material # 88b.

RESULTS AND INTERPRETATION

LITHOFACIES OF HOST ROCK

Eight lithofacies were identified based on depositional texture and fossil content. Refer to Table 1 for a summary of the facies

F1 - Mudstone

This light gray to buff mudstone is generally thinly bedded with bed thicknesses ranging between 10 and 20 cm. Diagenetic features such as stylolites and pressure solution seams separate some of the beds.

F2 – Cherty Mudstone-Wackestone

This facies is similar to F1 and exhibits similar characteristics except for that present within this facies are chert layers. The chert bands occur at intervals of about 0.5 – 1 m, with bed thickness of chert ranging between 10 and 30cm. The chert band is dark black to brown in color, and in thin section it is dominated by spicules.

F3 – Tan to dark brown shale

This facies is tan to dark brown in color. The shale is also friable, highly fissile and contains no fossils. The occurrence of this facies is restricted to one interval in the Medicine Lodge locality.

F4 – Wackestone

The wackestone facies is tan to brown with bed thickness ranging between 20 and 40 cm. Skeletal grains include crinoids, fenestrate bryozoans, gastropods, ostracods, foraminifera, algae and corals (Fig. 4A). Some of the grains have been recrystallized. Additionally, some silicification is observed within this facies as well as the presence of both open and filled (with calcite) fractures.

F5 – Packstone-Grainstone

This is the most common facies within the study area. The facies consist of light gray – whitish massive beds with thicknesses between 5 and 20cm, often separated by stylolites and pressure solution. Three types of grainstone could be distinguished within the study area.

F5.1 – Peloidal Packstone-Grainstone

This facies is composed of mostly peloids, with bioclast of brachiopods, bryozoan, ostracods and some benthic foraminifera (Fig. 4B). The peloidal grain size are sub-angular to rounded and have very little porosity.

F5.2 – Oolitic Packstone-Grainstone

This facies (Fig. 4C), composed predominantly of ooids and other micritized grains, also exhibits visible laminations. Most of the ooids here have been completely micritized or replaced. Other skeletal grains found in this facies are crinoids, brachiopods and bryozoans. Some of the replaced ooids have a layer of micrite coating

around them and are stained with iron. This facies is moderately to well sorted, with some porosity in vugs and open fractures. Within this facies are calcite filled fractures that cuts through the grains.

F5.3 – Crinoidal/skeletal Packstone-Grainstone.

This facies is whitish in color and exhibits a gray color upon weathering. The massive bedded packstone – grainstone of predominantly crinoids also contains other skeletal grains such as echinoid stems, foraminifera, corals, ostracods, brachiopods, bryozoans and some coated grains (Fig. 4D,E&F). This facies is moderately sorted with grain sizes ranging from coarse to fine and porosity if any limited to open fractures and vugs.

F6 – Stromatolite Bindstone

The stromatolite bindstone (Fig. 4G&H) that occurs the within the study area is greatly silicified and exhibits a change in morphology from laterally linked conophyton in the lower half into microbial laminate in the upper half. The stromatolites have been described as *Condonophyscus austini* (Enzl et al., 1996).

Table 1: Lithofacies description

Facies	**Description**
F1 - Mudstone	Light gray to buff color fine grain and structureless rock with some of the beds separated by stylolites.
F2 - Wackestone	Similar to F1 except contains chert layers. Skeletal grains are mostly spicules.
F3 - Shale	The tan to dark brown highly fissile and friable shale contains no fossils. Occurrence is restricted to one interval in the Medicine Lodge area.
F4 - Packstone-Grainstone	Tan to brown with bed thickness between 20-40cm. Skeletal grains include crinoids, fenestrate bryozoans, gastropods, ostracods, foraminifera, algae and corals.
F5.1 - Peloidal Packstone-Grainstone	Packstone – grainstone texture composed mostly of peloids with some skeletal grains within the matrix.
F5.2 - Oolitic Packstone-Grainstone	Facies is made up of mostly micritized and replaced ooids and other skeletal grains. Some ooids display an identifiable micritic ring of coating around them. It is moderately to well sorted
F5.3 - Crinoidal/skeletal Packstone-Grainstone	Facies is made up of crinoids, echinoid stems, foraminifera, corals, ostracods, brachiopod, bryozoan and other coated grains. It is whitish in color and exhibits a greyish color upon weathering.
F6 – Stromatolite binstone	The silicified stromatolite exhibits change morphology from laterally linked conophyton to microbial laminate.

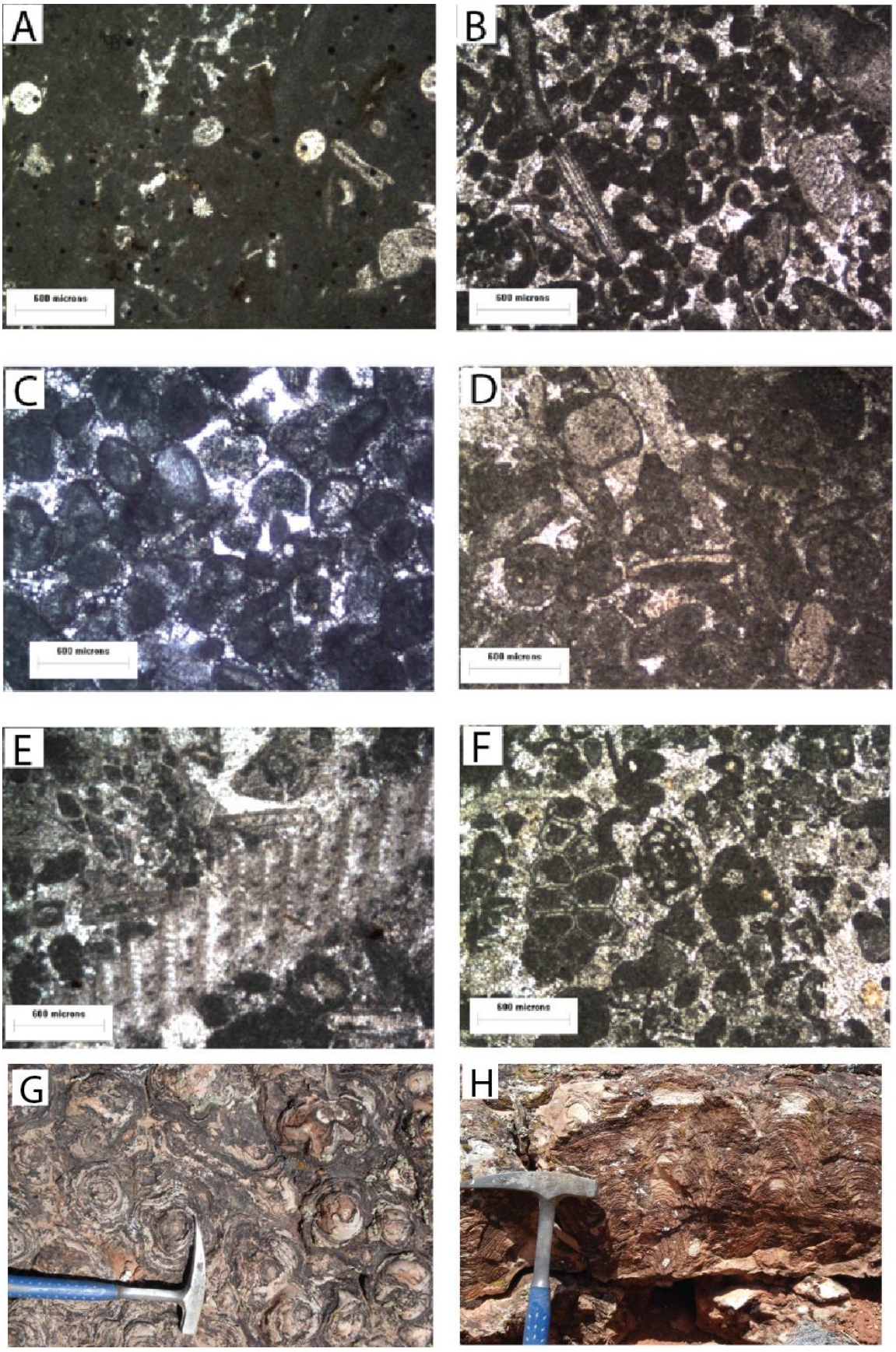
A
600 microns
B
600 microns
C
600 microns
D
600 microns
E
600 microns
F
600 microns
G
H

Fig. 4. Plane light photomicrographs of key facies and outcrop photos of stromatolite horizon. Note lack of porosity due to occlusion by cement. A – F4 facies from Medicine Lodge section three, with skeletal material including crinoids, echinoids and brachiopods. B – F5.1 facies from Shell Creek Canyon section, skeletal material seen here includes benthic foraminifera and crinoids. C – F5.2 facies from Medicine Lodge section one, note the miciritization of the ooids. D – F5.3 facies from Shell Creek Canyon section, skeletal grains seen here are brachiopods, crinoids, benthic foraminifera, bryozons, osctracods, some broken shell fragments and coated grains. E – F5.3 facies from White Creek Canyon section, skeletal grains seen here are brachiopods, crinoids, benthic foraminifera, bryozons, osctracods, some broken shell fragments and coated grains. F – F5.3 facies from Medicine Lodge section one, skeletal grains seen here are brachiopods, crinoids, benthic foraminifera, bryozons, osctracods, some broken shell fragments and coated grains. G&H are planar and transverse view of the stromatolite bed from sections in the White Creek Canyon. This laterally persistent stromatolite horizon has been described as *Condonophyscus austini* (Enzl et al., 1996) and serves a datum against which the depth of the karsting was measured.

LITHOFACIES INTERPRETATION

These facies described above are part of Sequence IV of the Madison Formation and herein interpreted as having been deposited on a shallow marine open to restricted lagoonal and peritidal setting. They have also been interpreted as recording the last shallowing upward phase of the succession before karstification (Sando, 1988). The interpretations of the facies were based on color, texture and fossil content.

F1 is interpreted to represent deposition in a low energy environment, and sparse bioclast within the facies could be indicative of high saline conditions making it difficult for organisms to thrive or live in.

F2 is interpreted to be deposited in a intertidal - subtidal area in a relatively fairly restricted environment, this interpretation is based on the presence of low fauna diversity. Additionally, the dominance of sponge spicules and lack of burrows are also suggestive of poor oxygenated water conditions.

F3 similar to F1 was deposited in a low energy environment. It's highly fissile nature with no fossils content, can be suggestive of anoxic water conditions making it difficult for organisms to thrive, or could have been deposited as a result of prolonged subaerial exposure. However, its brown color is consistent with an oxidizing condition and therefore most likely representative of subaerial exposure.

F4 similar to F2 was deposited in a low energy subtidal environment with possible fluctuating energy conditions. Absence of bioturbation within the facies may be indicative of the fact that the area wasn't conducive enough for organism to thrive in, which would suggest that the presence of open marine faunas within this facies were most likely brought in by periodic storms.

F5, F5.1, F5.2 and F5.3 contain a diverse biota consisting of crinoids, echinoids, bryozoans, brachiopods, corals, ostracods, ooids and other coated grains suggesting deposition under normal marine conditions. The environment was also subject to periodic wave action and high-energy conditions evident with the presence of ooids and other reworked grains. The extensive micritization of the skeletal grains and ooids, suggests that grains may have hard a long residue time post deposition.

Together, these facies presented show a restricted condition on a shallow shelf that was later on exposed and subjected to karst modification.

CARBON ISOTOPES

RESULTS AND INTERPRETATION

The matrix $\delta^{13}C$ values range from -4.1‰ to +2.2 ‰ VPDB. Within the sections measured, a systematic stratigraphic trend is evident, with $\delta^{13}C$ values generally increasing up section (Fig. 5). Medicine Lodge M1 is characterized by variable $\delta^{13}C$ values that range from -2.3 to + 0.7 ‰ and shows an increasing trend up section. This trend is consistent with the other two Medicine Lodge sections which both exhibit similar patterns. The $\delta^{13}C$ values of Medicine Lodge M2 ranges from -2.2 to -0.5 ‰ while Medicine Lodge M3 $\delta^{13}C$ values ranges from -2.7 to + 0.8 ‰. Shell Creek Canyon section exhibits similar patterns to M1 and M3 with $\delta^{13}C$ values that ranging from -2.9 to + 0.9 ‰. Finally, the White Creek Canyon section, exhibits the most variable $\delta^{13}C$ values, it range from -4.1 to + 2.20 ‰ and exhibit as well a general upward increasing trend.

Since carbon isotopic values record fluctuations in climate, oceanography, and sea level (Kump and Arthur, 1999; Saltzman, 2003) they can be traced globally and used for correlation and approximate age determination because the variations they record are unique to particular geologic periods. As a result they are widely used as a correlation tool and for understanding paleoenvironmental trends (Saltzman, 2003). For the mid-Carboniferous, the nature and timing of these isotopic shifts are well understood and have been defined at the Global Boundary Stratotype Section and Point (GSSP) in Arrow Canyon, NV (Saltzman, 2003). The $\delta^{13}C$ values of Arrow Canyon show a systematic variation with depth, the values begin at about 0.5‰ and show a distinct positive shift up to about 7‰ in the Early Mississippian. Additionally, the data also show a significant negative shift of $\delta^{13}C$ values in the latest Kinderhokian and Osagean, which have been interpreted to result from the subaerial exposure during the latest Mississippian (Saltzman, 2013; Koch et al., 2014).

The $\delta^{13}C$ values (Appendix 1) were plotted against the measured sections to aid in the correlation between the measured sections (Fig. 6). Additionally, these values can be used to estimating the timing of the subaerial exposure, although lack of adequate age control within the Madison made it difficult to ascertain the onset of the unconformity from the isotopic shifts. Even though the lack of age control within the data makes it difficult to directly correlate it with the GSSP of Arrow Canyon, the isotopic trend seen in the sections in the Madison Formation are comparable to that of Arrow Canyon. From those shifts, an estimate for the age of the Madison exposure is around mid Osagean. The $\delta^{13}C$ values of the Madison Formation show a systematic variation with depth as well. The data show negative shift of about -2.0 ‰ towards the top of the top of the section.

These values are also comparable with other studies of similar time interval in the Midcontinent U.S. and elsewhere (Mii et al., 1999; Grossman et al., 2008; Koch et al, 2014). These shifts in $\delta^{13}C$ to negative values towards the top of the sections are representative of the subaerial exposure at the top of the Madison that subjected the rocks to meteoric diagenesis.

Fig. 5: NW-SE Cross-section showing stratigraphic sections and carbon isotope profiles. Also shown are shallowing upward sequences (black triangles).

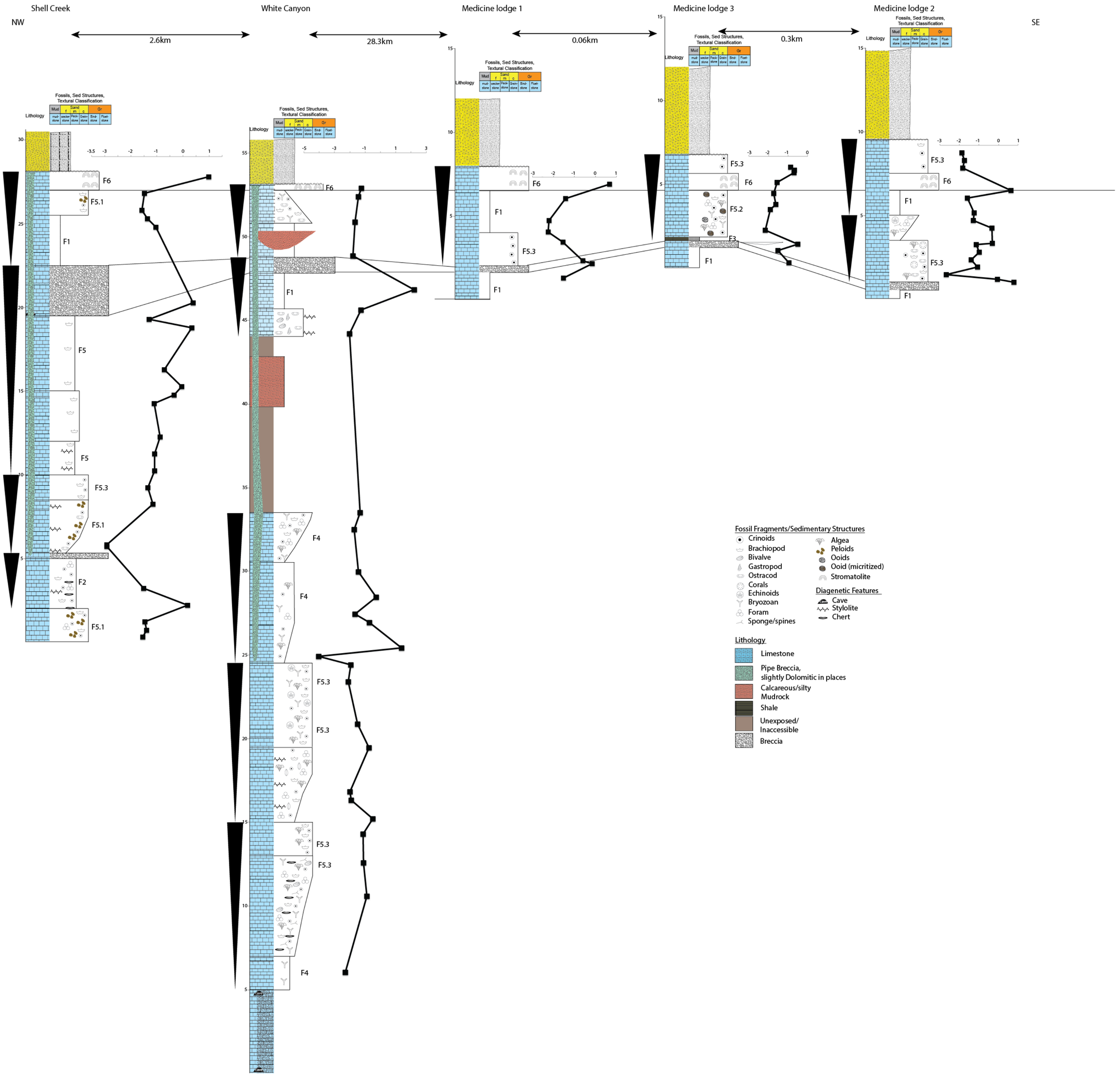
Shell Creek
White Canyon
Medicine lodge 1
Medicine lodge 3
Medicine lodge 2
NW
SE
2.6km
28.3km
0.06km
0.3km
Fossils, Sed Structures, Textural Classification
Lithology
Mud
Sand
Gr
f
m
c
mud-stone
wacke-stone
Pack-stone
Grain-stone
Bind-stone
Float-stone
F6
F5.1
F1
F5
F5.3
F2
F4
F5.2
F3
Fossil Fragments/Sedimentary Structures
Crinoids
Brachiopod
Bivalve
Gastropod
Ostracod
Corals
Echinoids
Bryozoan
Foram
Sponge/spines
Algea
Peloids
Ooids
Ooid (micritized)
Stromatolite
Diagenetic Features
Cave
Stylolite
Chert
Lithology
Limestone
Pipe Breccia, slightly Dolomitic in places
Calcareous/silty Mudrock
Shale
Unexposed/ Inaccessible
Breccia

KARST FEATURES

DESCRIPTION

Besides the sheer cliff exposures exhibited by the Madison Formation, one of its most striking features is the extensive breccias, paleocaves and pipes/sinkholes that occur below the unconformity that caps the formation (Figs. 6-11). Described below are the various karst features of the study area.

Breccias

Two types of breccia are identified within the study area based on the composition of the matrix. A red, fine-grained matrix characterizes one type, while the other contains a gray matrix. These breccias are located either in laterally extensive beds or in vertical solution pipes/sinkholes and paleocaves (fig. 6-11).

Gray matrix breccia

This breccia contained in a gray matrix is stratiform (Fig. 6A&B); The gray matrix breccia interval is stratigraphically bounded above and below by unaltered strata, has a relatively flat base and a highly irregular roof (Fig. 8 – 11). It is widely distributed and can be traced from section to section throughout the study area (Fig. 8 – 11). This highly chaotic breccia is composed of angular clasts of cobble-to boulder-size blocks from the surrounding limestone beds (Fig. 6 A&B). Depending on location, this breccia exhibits both matrix and clast supported fabrics (Fig. 6 A&B). The composition of the matrix when present is fine-grained calcite micrite.

Red, fine-grained matrix breccia

This breccia occurs mostly in vertical pipes/sinkholes or paleocaves. It is highly monomictic, chaotic and made up of unsorted angular clasts consisting of cobble-to-boulder-sized limestone blocks contained within a red, fine-grained matrix. It is also texturally variable in that it exhibits both matrix (Fig. 6C &D) and clasts (Fig. 6E) supported fabrics depending on location as can be seen in Figs. 6 C-E. When occurring in pipes/sinkholes, the matrix content generally decreasing from top of the to more clast supported further down in the pipes. The composition of the matrix is red, fine-grained silt/sand as seen in Fig. 6F from the overlying Darwin Sandstone.

Paleocaves

The paleocaves occur extensively throughout the field area (Fig. 7&10). They range in size from a few centimeters up to tens of meters and show no predictive pattern in that they are not restricted to a particular stratigraphic level or occur all at the same interval. However, in some instance as can be seen in Fig. 7, the caves occur at or near the same stratigraphic interval. The base of some of the caves are filled with breccia; typically red matrix, while in some instances they are empty.

Sinkholes/Pipes

The pipes/sinkholes within the study area extend from the top of the unconformable surface between the Madison and Amsden Formations (Fig. 8). These pipes/sinkholes, typically filled with red, fine-grained matrix beccias, penetrate down into the Madison limestones. They measure as much as 20 and 30 m deep and about 12 m wide at Shell and White Creek Canyon, respectively. Just like the paleocaves, the pipes/sinkholes do

not occur within a particular set of interval or distance and show no predictable pattern in their occurrence.

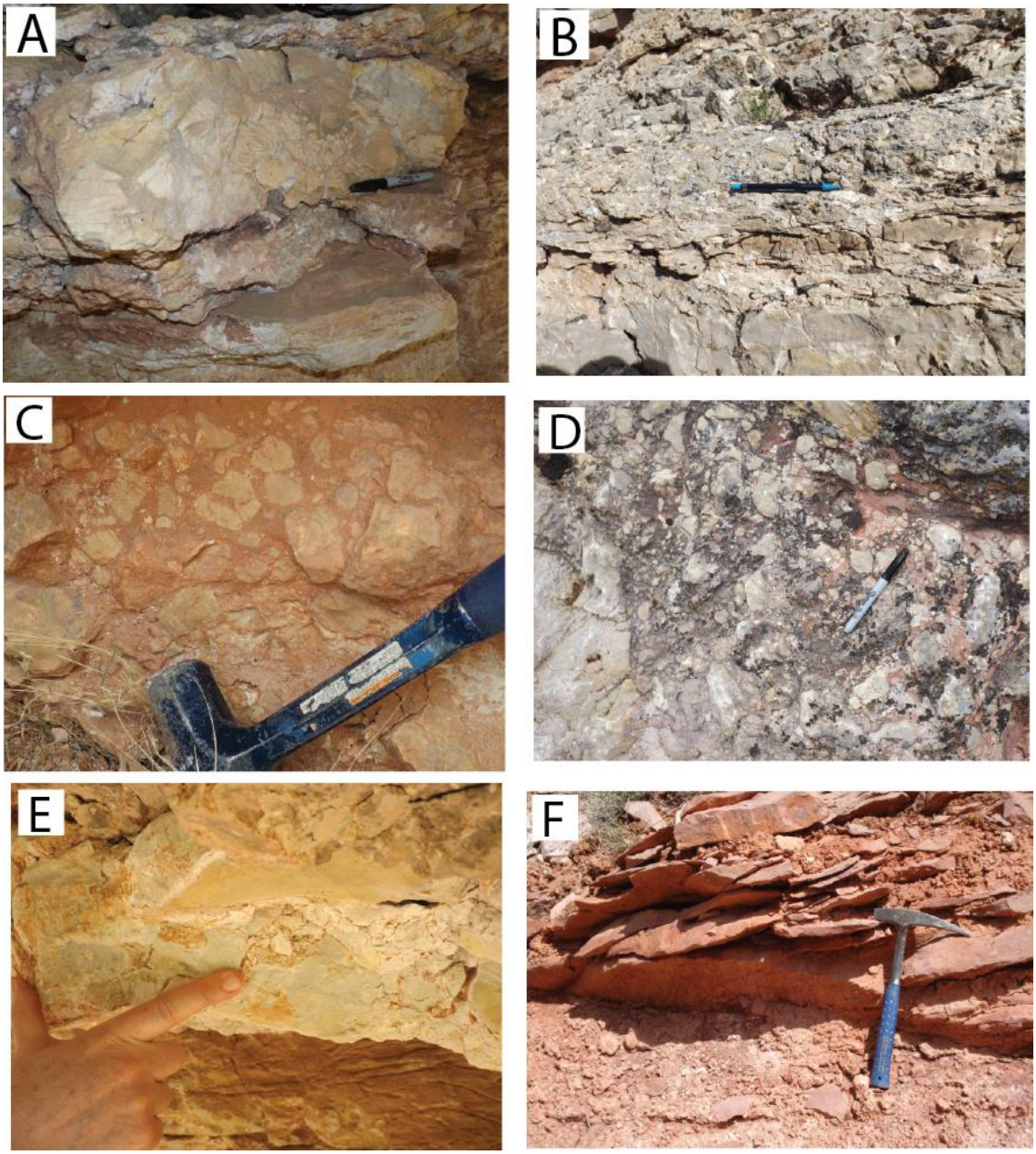

Fig. 6: Outcrop photos of the two types of breccias seen in the study area. A is outcrop photos from Medicine Lodge of matrix supported fabric of the gray breccia while B is

outcrop photo from section in White Creek Canyon of clast supported fabric of the gray breccia. E – outcrop photo from Shell Creek Canyon section of matrix support fabric of the fine, red-grained breccia. F – outcrop photo from Medicine Lodge section of clast supported fabric of the fine, red-grained breccia. G - outcrop photo from White Creek Canyon section of matrix support fabric of the fine, red-grained breccia. H – outcrop photo of photo from White Creek Canyon section of the red matrix of solution pipe infilling.

Fig. 7: outcrop photo from the Bighorn Canyon recreational area of a cave system developed below the Madison unconformity surface (Mississippian – Pennsylvanian unconformity). Seen here is the spatial distribution of the caves as well as the varying sizes of the caves. Strata ranging from few centimeters to tens of meters separate the caves which can be up to about 5 m high.

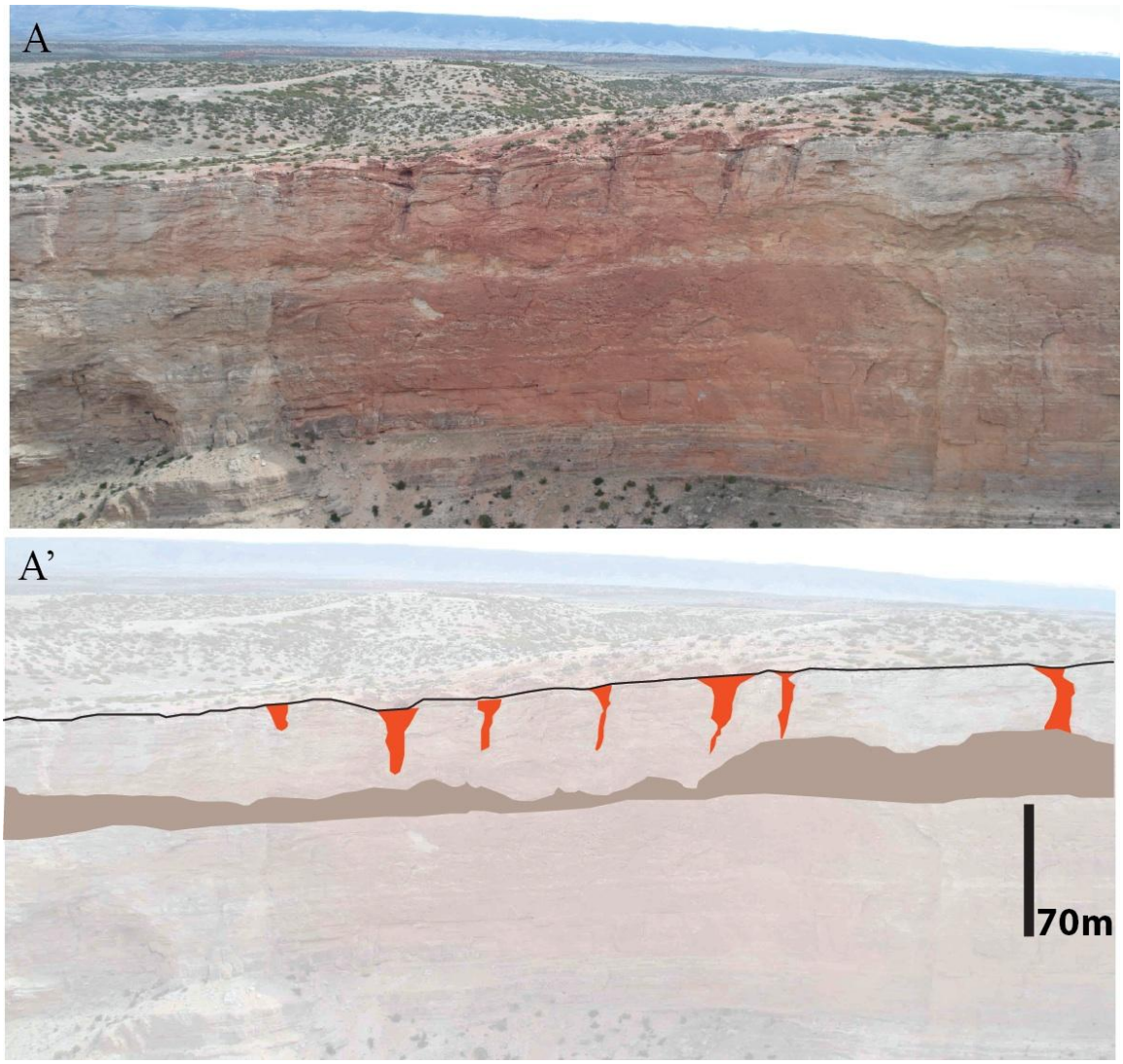

Fig. 8: Interpreted outcrop panels taken around Bighorn Canyon recreation area, showing some of the spatial distribution and relation between the pipes/sinkholes (red) and bedded (gray) breccias.

Fig. 9: Interpreted outcrop panel taken at Medicine Lodge, showing the bedded breccia.

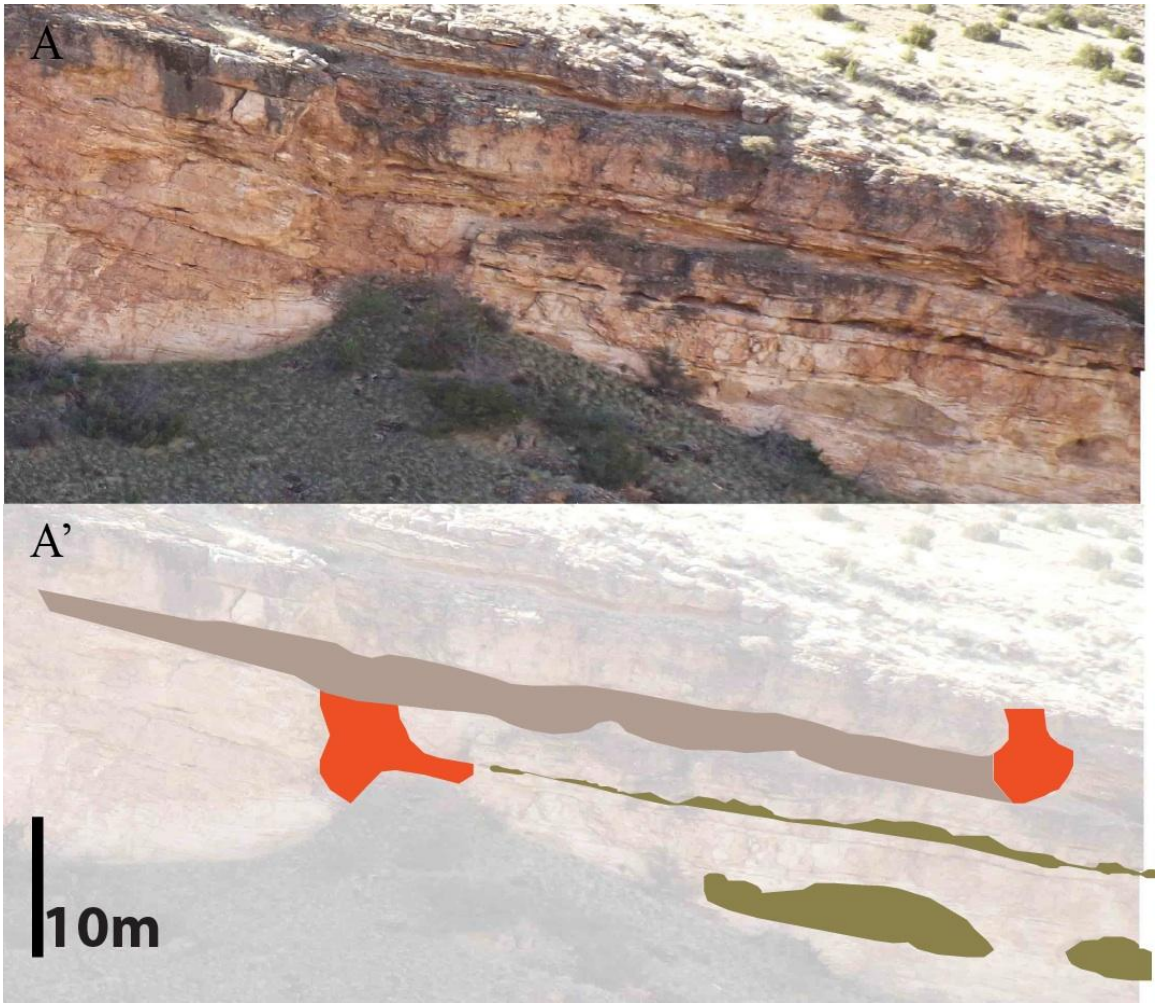

Fig. 10: Interpreted outcrop panels taken Shell Creek Canyon, showing some of the spatial distribution and relation between the pipes/sinkholes (red) and bedded (gray) breccias. Also seen here are the paleocaves (green).

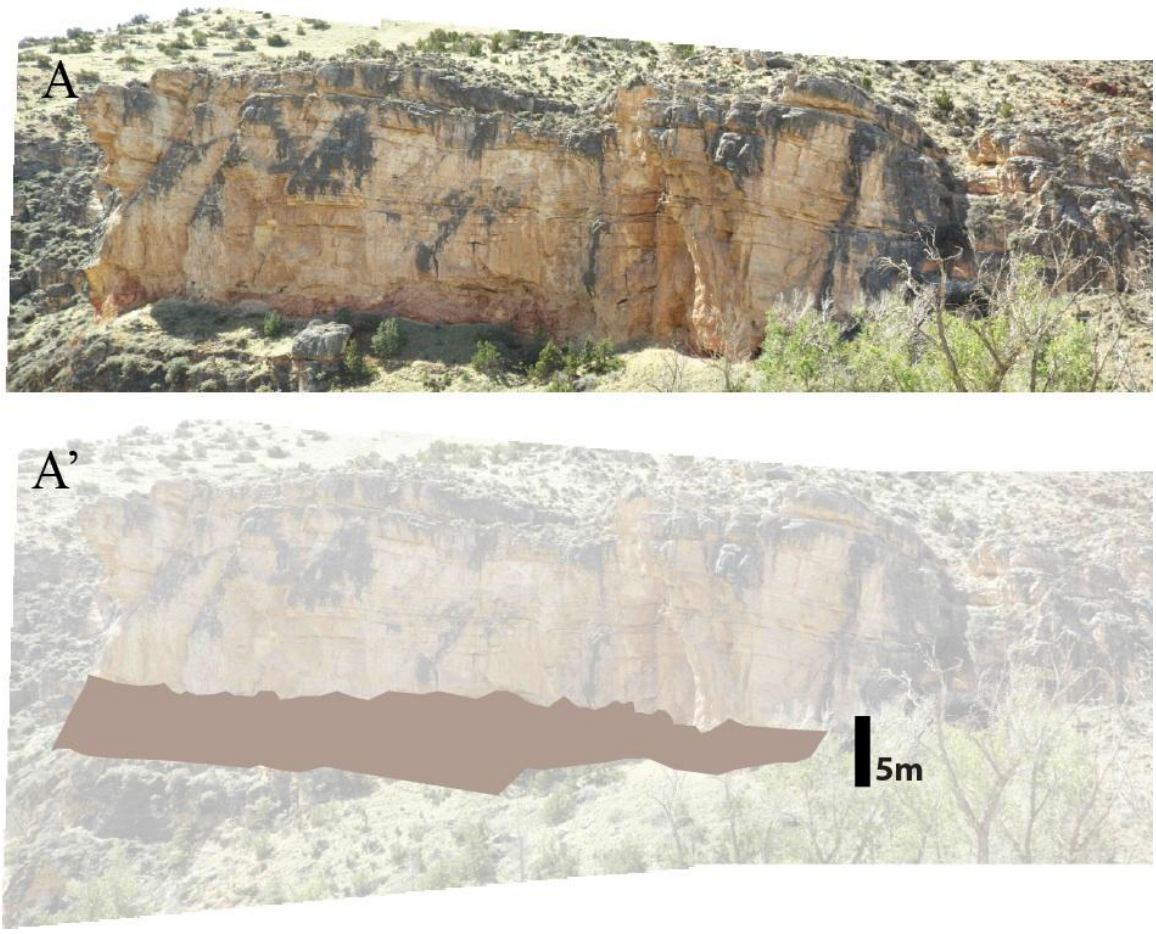

Fig. 11: Interpreted outcrop panels taken at White Creek Canyon, showing the bedded breccia.

INTERPRETATION

The Madison breccias and solution zones within the field area has also been mapped out in other locations throughout the Bighorn Basin by previous workers (Sando, 1974, 1988; Sonnenfeld 1996a; Kloss, 2011) and are interpreted to have formed from evaporite dissolution during the subaerial exposure of the platform. Even though no evaporite were seen during field measurement, previous studies by Severson (1952) and Andrichuk (1955) have correlated the lower Madison breccias to equivalent evaporite bed in the subsurface at Williston Basin and outcrop breccias within the Madison in Montana to equivalent stratigraphic layer of anhydrite intervals in the subsurface respectively. The absence of evaporite on the surface in the field area is reflective of the long exposure period of the platform that subject it to complete dissolution by meteoric diagenesis.

Evaporite-collapse breccias are formed from the removal/dissolution of salts, and in the process, the gravitational collapse of the overlying (overburden) rock (Warren, 1999). Formation of this type of breccia is usually associated with exposure of the evaporite interval, as a result of retreating baseline (Loucks, 1999). Breccias typically interpreted as solution collapse breccia have sharp basal contacts, irregular tops and exhibit inverse grading (Warren, 1999; Elaissen and Talbot, 2005).

These descriptions are consistent with the gray matrix breccia encountered in the Madison Formation, suggesting it was formed via solution-collapse process. Additionally, the sharp basal contact, irregular top seen within the study area (Fig. 8) are consistent with the removal of an evaporite bed that was deposited throughout the basin by dissolution induced by percolating meteoric waters when the platform was exposed. Also, XRD analysis of the clay within the Madison breccia by McCaleb and Wayhan

(1986) and Vice (1988) shows that the clays within the breccia are mostly illite. Illite as suggested by Roberts (1966) is common clay in evaporite-collapse breccia as opposed to soil-related breccia (Demiralin et al., 1993).

After the formation of the stratiform breccia, the red, fine-grained matrix breccia was formed within the pipes created. The red, fine-grained matrix comes from the overlying Darwin Sandstone.

As stated earlier, reconstruction of how these karst features are formed are essential especially for reservoir evolution. Based on this and the evidence presented above, the formation of the karst features can be explained in a series of four stages from the observed sedimentologic features in the field, including petrographic and isotopic analysis. Previous study by Kloss (2011) of karst within the Bighorn Canyon in north central Wyoming and proposed a stepwise model for the evolution of the Madison karst as well. Although our models do not remarkably disagree with each other, they both shed light on the complexities and great heterogeneity that is often expressed by karsted carbonates systems and further illustrates some key differences within the area.

Stage A (Fig. 12A) is the pre-karstification stage; this is before the exposure of the platform that subjected it to dissolution by meteoric water. First there was the deposition of Lower Madison Limestone, followed by a lower evaporite layer and then the middle Madison and an upper evaporite layer which was subsequently bounded above by more Limestone, a stromatolite layer and final phase of Madison deposition. Evidence for more Madison deposition post stromatolite horizon can be seen in the Medicine Lodge section 3 (refer to Fig. 5).

After deposition, Stage B follows with the exposure of the Madison platform and onset of karstification (Fig. 12B). Meteoric water began the dissolution of the surface and creation of pipes, which have been described by Sando (1988) to serve as paleohydrologic conduits for the meteoric fluids from the surface down into the limestone strata and evaporite beds. This facilitated the dissolution of the limestone and the evaporite bed and began the set of the formation of the gray matrix breccia

Long-term exposure of the platform resulted in increased karstification and modification of the rocks. The pipes expanded and were became wider as illustrated in Stage C. Within this stage as well was the deposition of the Darwin Sandstone, thus the pipes formed not only served as paleohydrologic conduits, but also as sediment pathways, filtering Darwin Sandstones and commencing the formation of the red matrix breccia. The prolonged exposure of the Madison platform also subjected the top of the Madison Limestone to increased erosion, which lead to the creation of a more pronounced irregular surface evident with the uneven erosion. Using the stromatolite as a marker horizon, the depth of karsting and erosion was determined relative to that layer. A crinoidal grainstone lies atop the stromatolite bed in two of the measured sections in Medicine Lodge (Fig. 5 and see appendix for details on the measured sections) and is completely missing in other localities less than 1km apart. Meanwhile in Shell and White Creek Canyons, the stromatolite serves as the unconformable surface with the Darwin sandstone. This suggests the creation of regional topographic relief of about 3 m on the unconformable surface.

Finally stage D (Fig.12D) represents the complete development of the karst system in the Madison Formation.

Fig. 12: A schematic illustrated model for karstification of the Madison Formation (not drawn to scale). A – represents the initial surface of the Madison after deposition and before it was subaerially exposed. B – illustrates the initial dissolution and development of an irregular terrain as well as solution pipes/sinkholes as result erosion from subaerial exposure of the platform. C – illustrates the onset of deposition of the Darwin Sandstone and enhanced growth of the solution features with initial formation of both breccias. D – illustrates the full development of the Madison karst system.

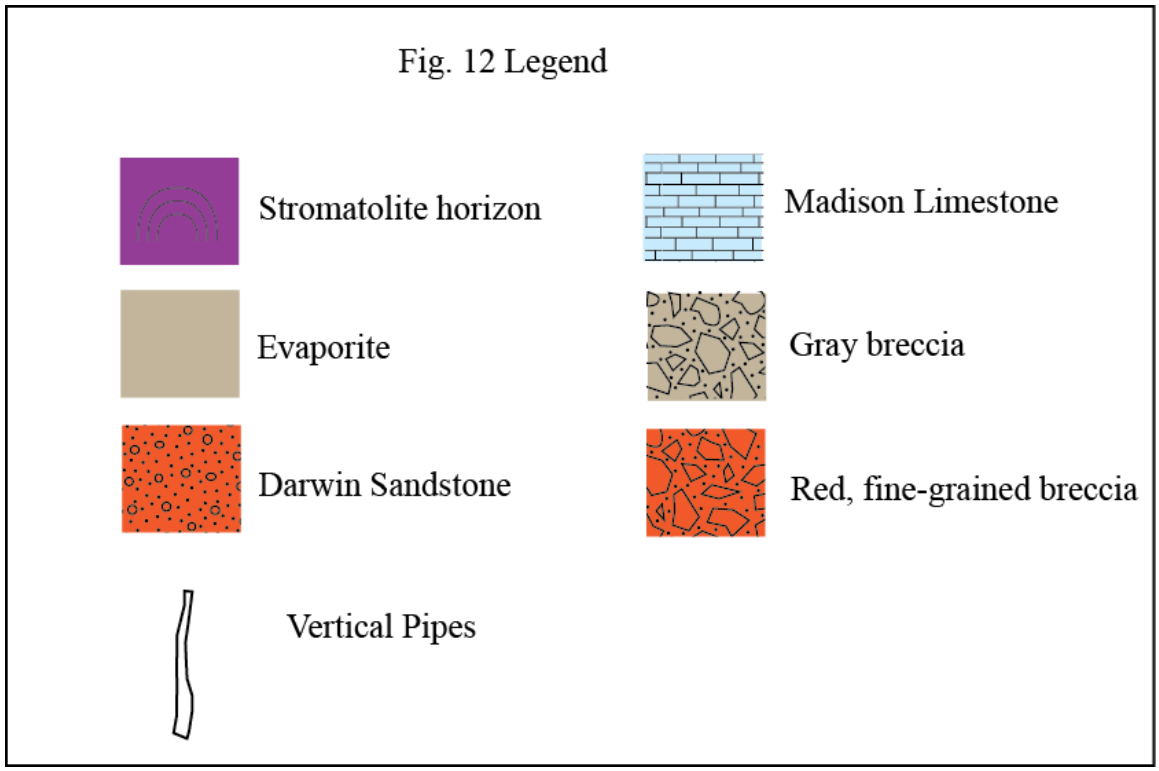

Evolution of the Madison karst.

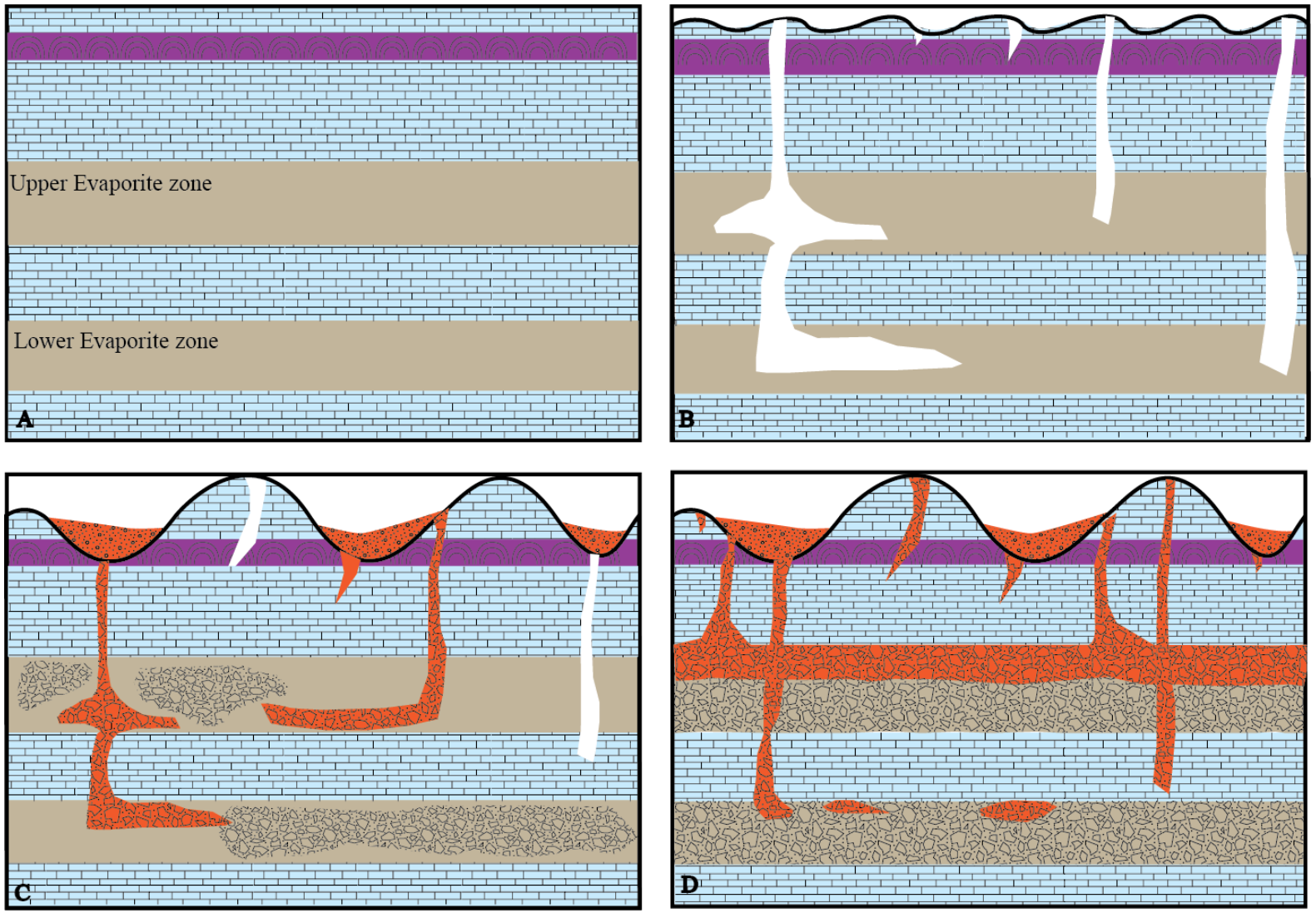

IMPLICATIONS FOR RESERVOIR PROPERTIES

Karsted limestones pose challenges in reservoir modeling because they can hinder both porosity and permeability of the rocks and as well as create lateral heterogeneity that often results in compartmentalization of the reservoir (Esteban and Wilson, 1993; Kerans, 1997; Buschkuehle et al., 2007). Additionally, karsting has been shown to affect both reservoir thickness and seal effectiveness (Dembicki and Machel, 1996). The duration of exposure also plays an important role in affecting reservoir properties (Purdy and Waltham, 1999; Saller et al., 1999).

Madison breccias within the field area was formed during prolonged subaerial exposure that lasted anywhere from 10-34 m.y. Such long time duration for karst development would have promoted meteoric cementation of the host, thereby lowering the porosity of the host rock (Fig. 8). As a result, the host can serve as a viable seal for the reservoir. Additionally, the karst pipes and solution breccias formed, showed great variability in their composition in that they display both clast and matrix supported fabric, as well as lateral heterogeneity due to uneven distribution of karst features, thus attest to the potential heterogeneity that could exist within the reservoir. Additionally, the paleocaves, which can serve for cavernous porosity range in size from few centimeters to tens of meters and are separated by unaltered strata, don't all occur at the same stratigraphic horizon. This, coupled with the lateral variability of the pipes/sinkholes and solution breccia, can lead to reservoir compartmentalization; creating isolated pockets/intervals of pay zone separated by strata of mudstone-wackestone to grainstone texture of low porosity and permeability, which can serve as seal or flow barrier. The heterogeneity and spatial variation expressed in the Madison Formation of the Bighorn

Basin are similar to other karsted reservoirs in the China in the Tahe oil fields and Tarim basin thus suggesting that the Madison karst can indeed serve as a viable model for examples in the subsurface. Therefore, understanding these heterogeneities prior to development, will aid in building more realistic reservoir model as well as providing a more realistic estimation of volumetric reserves.

CONCLUSIONS

The Mississippian Madison Formation in the Bighorn Basin of northeastern Wyoming is capped by an extensively karsted horizon created by subaerial exposure of the Madison platform. The prolonged exposure of the platform resulted in solution enhanced features, including pipes/sinkholes, paleocaves, and stratiform breccias. Two types of breccia are present; a red, fine-grained matrix breccia and a gray matrix breccia. The gray matrix breccia is stratiform, while the red, fine-grained matrix breccia is typically found in vertical solution pipes/sinkholes. Both breccias show great variability in that they are both clast and matrix supported. The vertical solution pipes/sinkholes measured as much as 12m wide and 20-30m deep and filled with collapse breccia of cobble-to-boulder size blocks in a red fine-grained matrix, while the paleocaves range in size from few centimeters to tens of meters and separated by unaltered limestone strata of low porosity and permeability. Such variability can lead to compartmentalization of reservoirs with the surrounding serving as a seal/flow barrier due to their low porosity and permeability. This indicating that proper understanding of such lateral heterogeneity and uneven karst features are essential when evaluating reservoirs and thus the exposed

karsted horizon atop the Madison can serve as viable analog for assessment of reservoirs in the subsurface.

ACKNOWLEDGMENTS

This research was supported by NSF Grant EAR-0645504 to T. Frank and GSA grant to L. Nana Yobo. We are grateful to the Flitner family for access to White Creek Canyon. Stable isotope analyses were carried out at Keck Paleoenvironmental and environmental laboratory at the University of Kansas.

APPENDIX

1. Detailed graphic log of measured sections

Medicine Lodge 1
0 - 15m
Location ° 0297496
4910285

Madison Formation
Mississippian
Bighorn Basin, WY

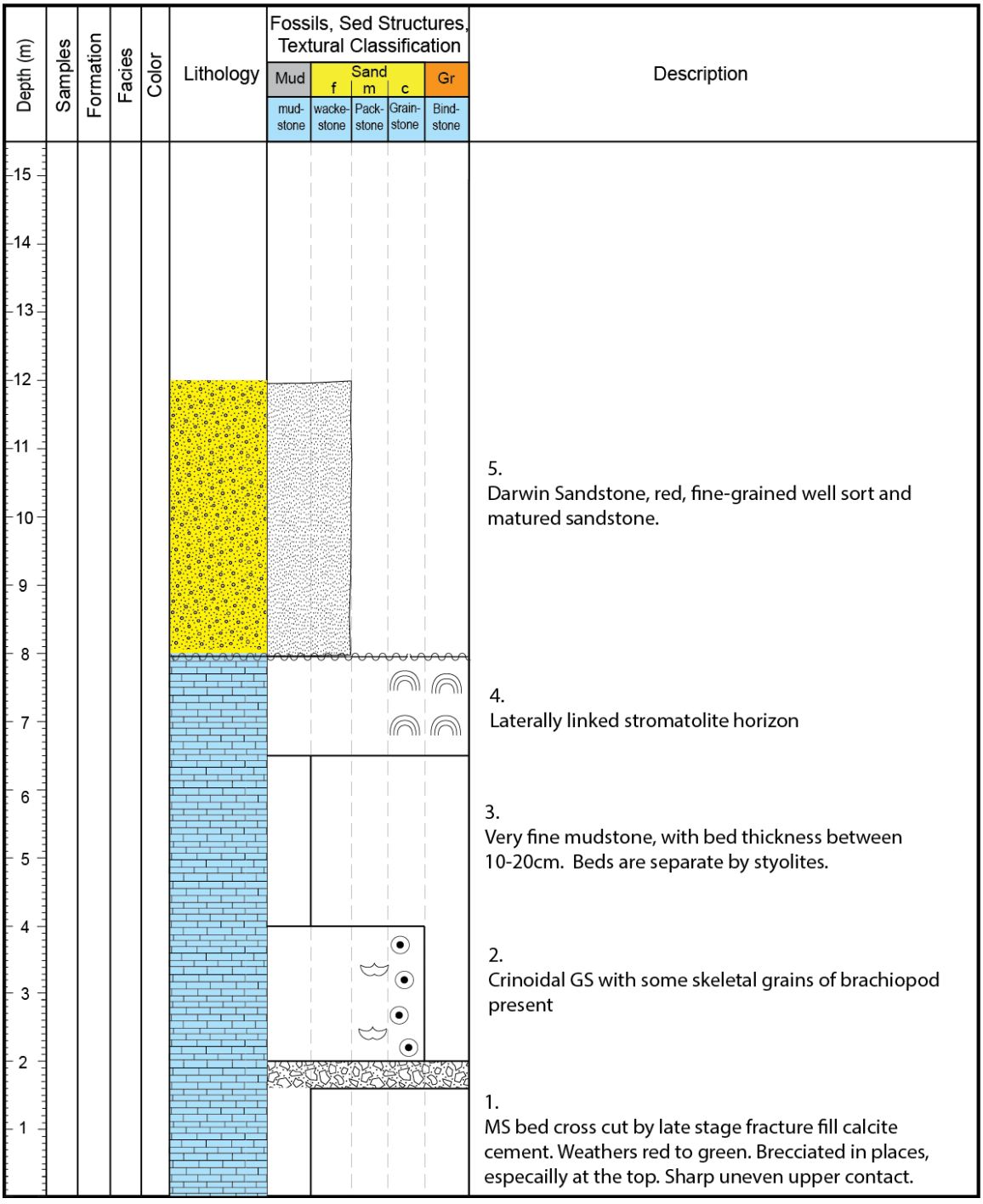

Medicine Lodge 2
0-15m
Location ° 0297332
4910523

Madison Formation name
Mississippian
Big Horn Basin, WY

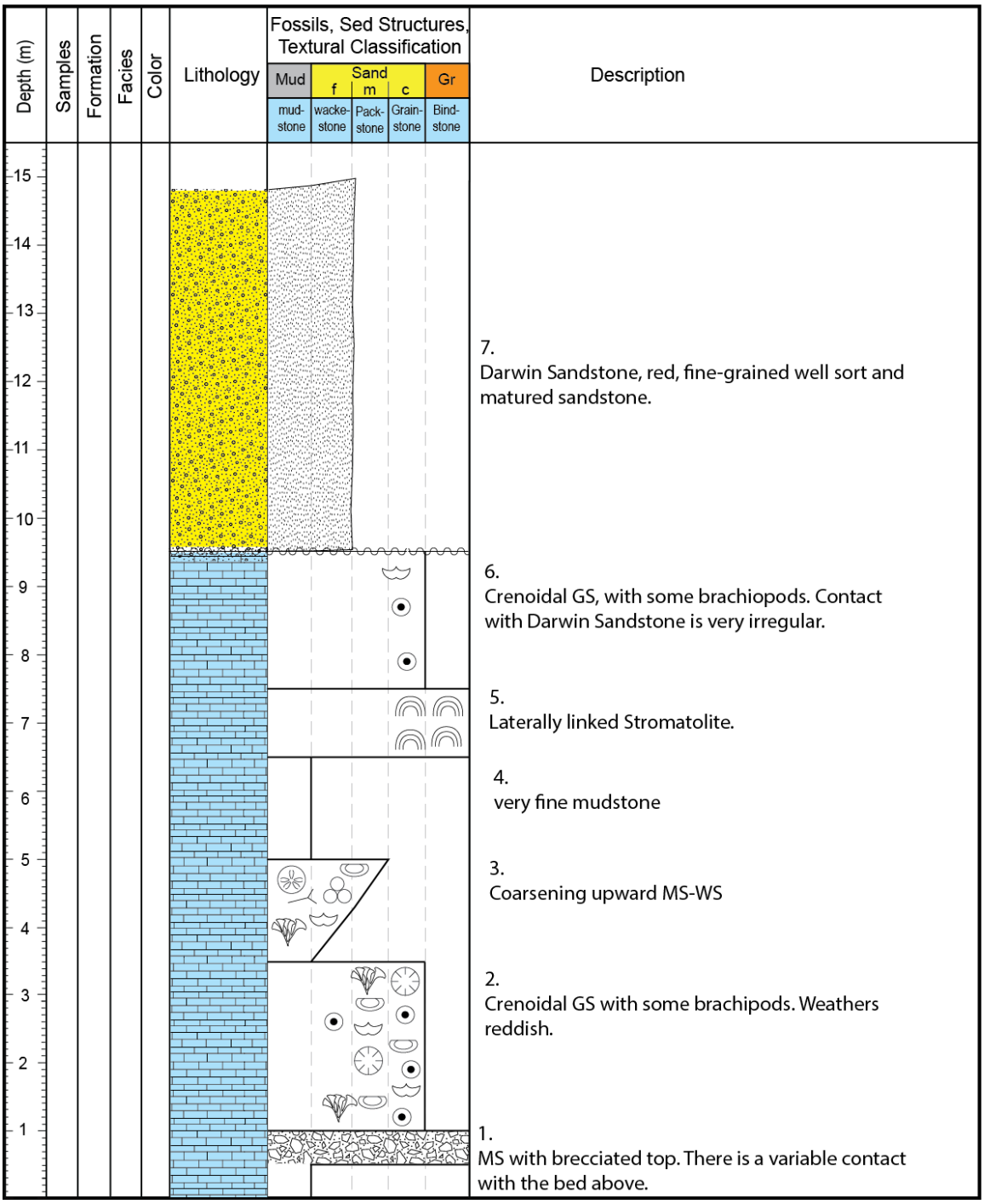

Medicine Lodge 3
0-15m
Location ° 13T 0297286
4910564

Madison Formation
Mississippian
Big Horn Basin, WY

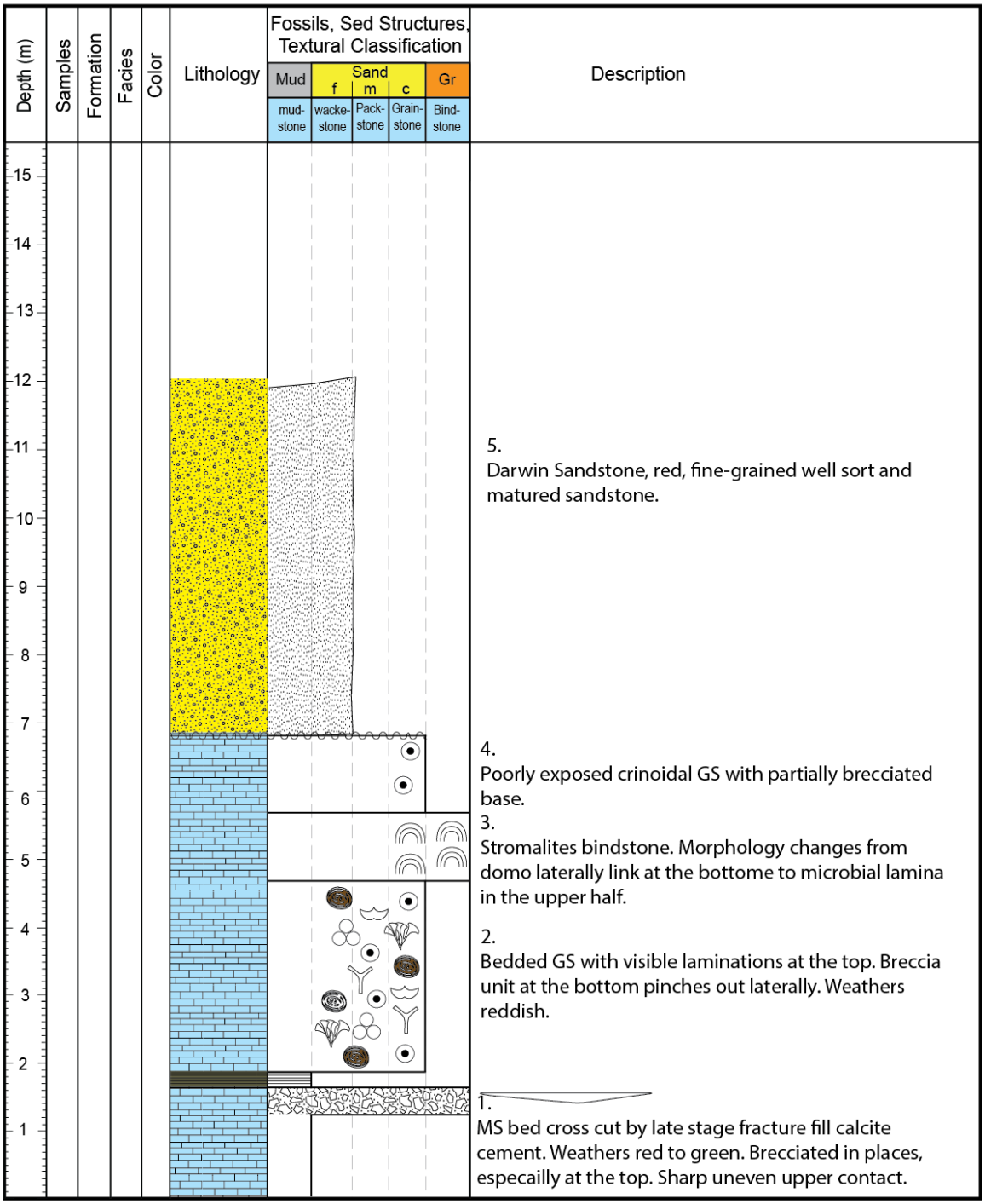

Shell Creek
0.0 - 15.0 m
Location ° 0284947
4938768

Madison Formation
Mississipian
Big Horn Basin, WY

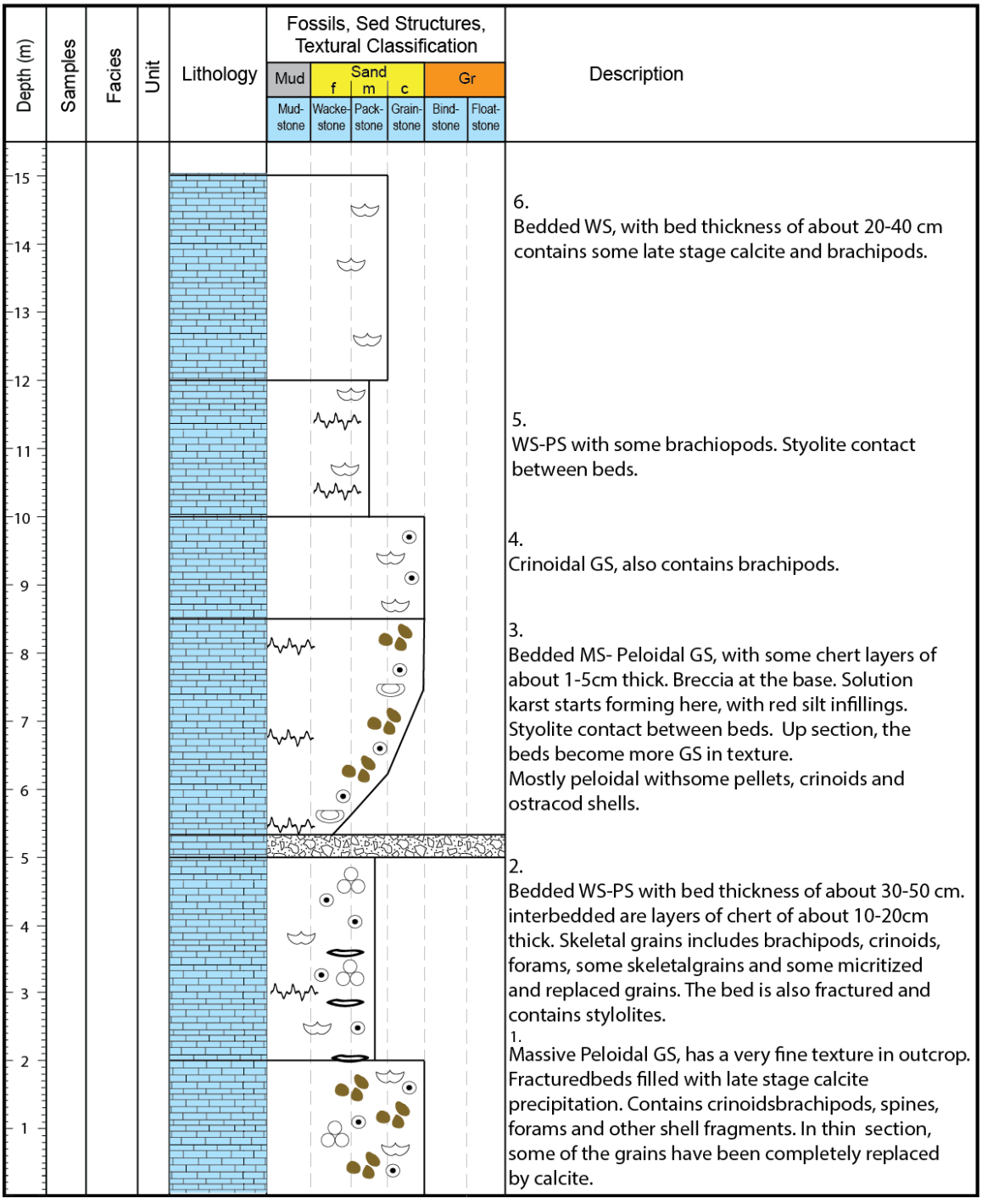

6.
Bedded WS, with bed thickness of about 20-40 cm contains some late stage calcite and brachipods.

5.
WS-PS with some brachiopods. Styolite contact between beds.

4.
Crinoidal GS, also contains brachipods.

3.
Bedded MS- Peloidal GS, with some chert layers of about 1-5cm thick. Breccia at the base. Solution karst starts forming here, with red silt infillings. Styolite contact between beds. Up section, the beds become more GS in texture.
Mostly peloidal withsome pellets, crinoids and ostracod shells.

2.
Bedded WS-PS with bed thickness of about 30-50 cm. interbedded are layers of chert of about 10-20cm thick. Skeletal grains includes brachipods, crinoids, forams, some skeletalgrains and some micritized and replaced grains. The bed is also fractured and contains stylolites.

1.
Massive Peloidal GS, has a very fine texture in outcrop. Fracturedbeds filled with late stage calcite precipitation. Contains crinoidsbrachipods, spines, forams and other shell fragments. In thin section, some of the grains have been completely replaced by calcite.

Shell Creek
15.0 - 30.0 m
Location ° 0284947
4938768

Madison Formation
Mississipian
Big Horn Basin, WY

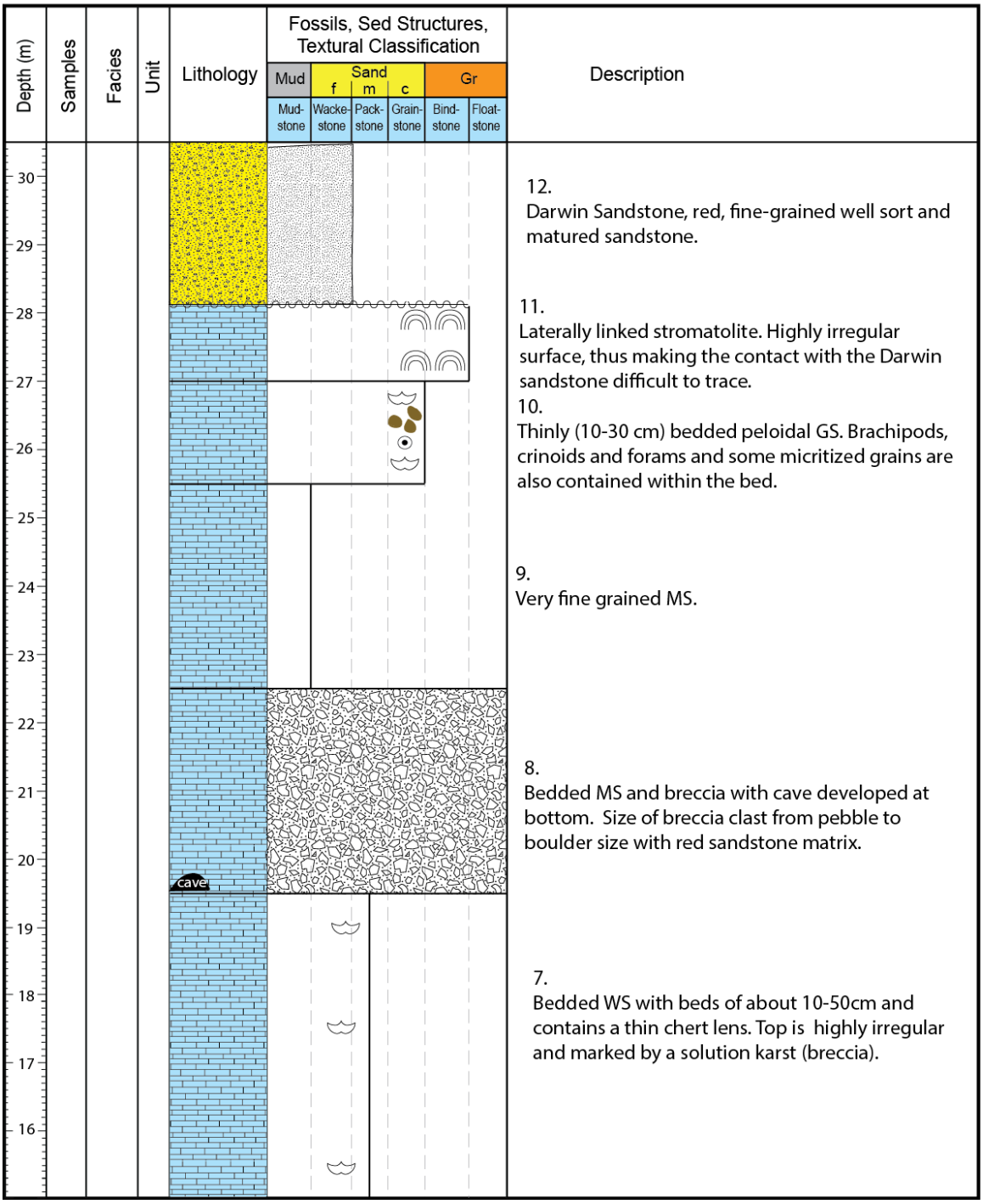

12.
Darwin Sandstone, red, fine-grained well sort and matured sandstone.

11.
Laterally linked stromatolite. Highly irregular surface, thus making the contact with the Darwin sandstone difficult to trace.

10.
Thinly (10-30 cm) bedded peloidal GS. Brachipods, crinoids and forams and some micritized grains are also contained within the bed.

9.
Very fine grained MS.

8.
Bedded MS and breccia with cave developed at bottom. Size of breccia clast from pebble to boulder size with red sandstone matrix.

7.
Bedded WS with beds of about 10-50cm and contains a thin chert lens. Top is highly irregular and marked by a solution karst (breccia).

White Canyon
0.0 - 15.0 m
Location ° 0285189
4936284

Madison Formation
Mississippian
Big Horn Basin, WY

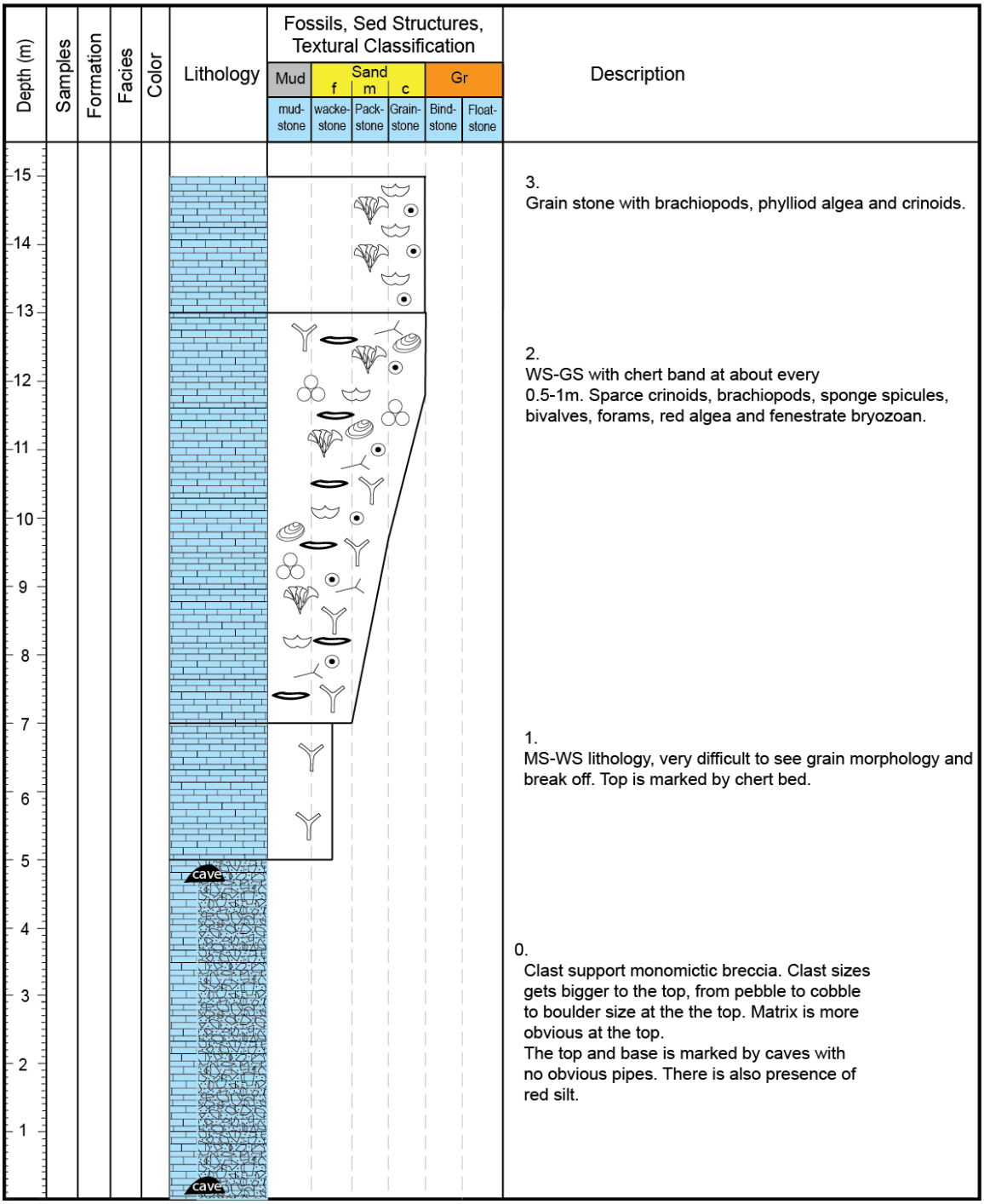

White Canyon
15.0 - 30.0 m
Location ° 0285189
4936284

Madison Formation
Mississippian
Big Horn Basin, WY

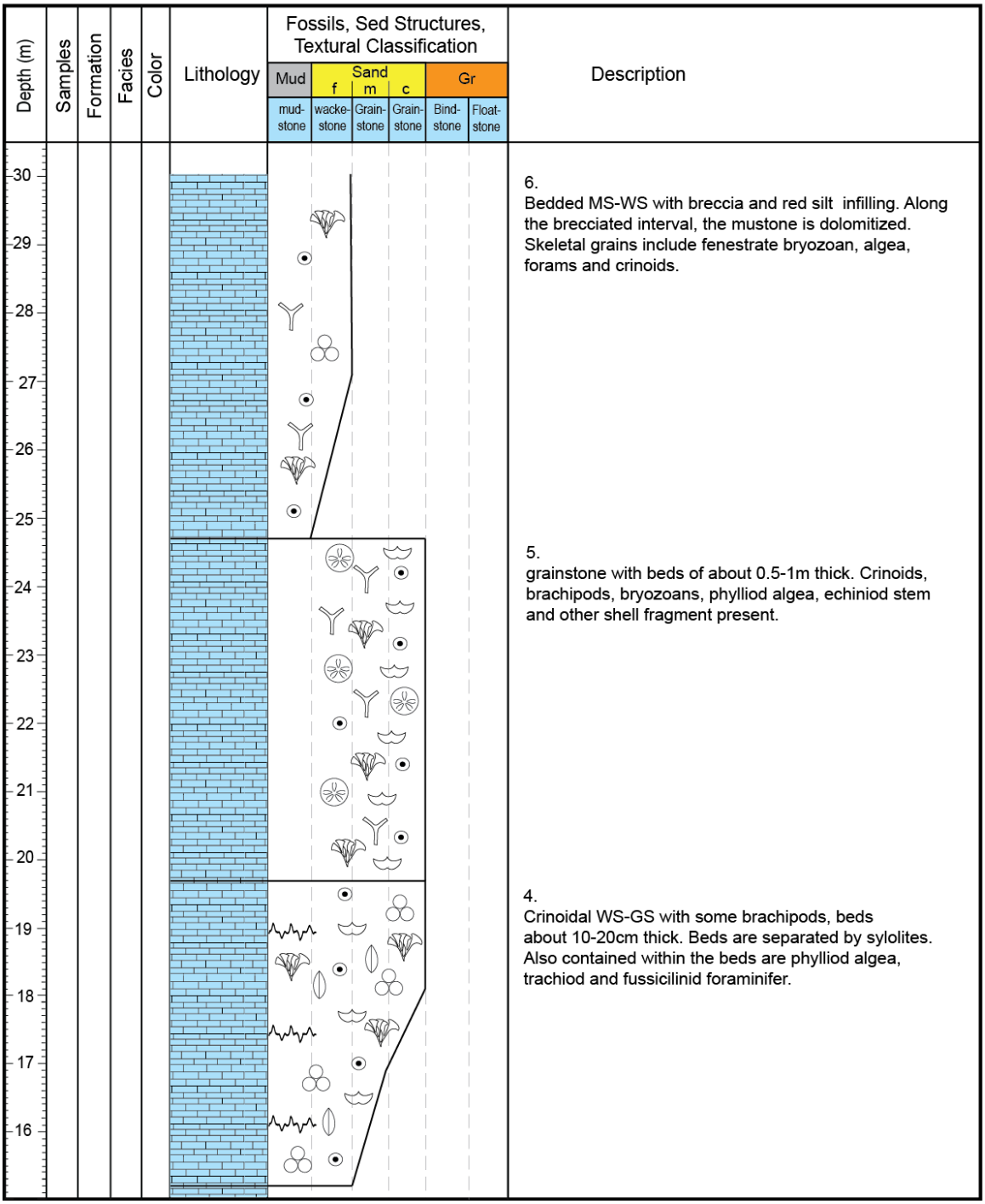

White Canyon
30.0 - 45.0 m
Location ° 0285189
4936284

Madison Formation
Mississippian
Big Horn Basin, WY

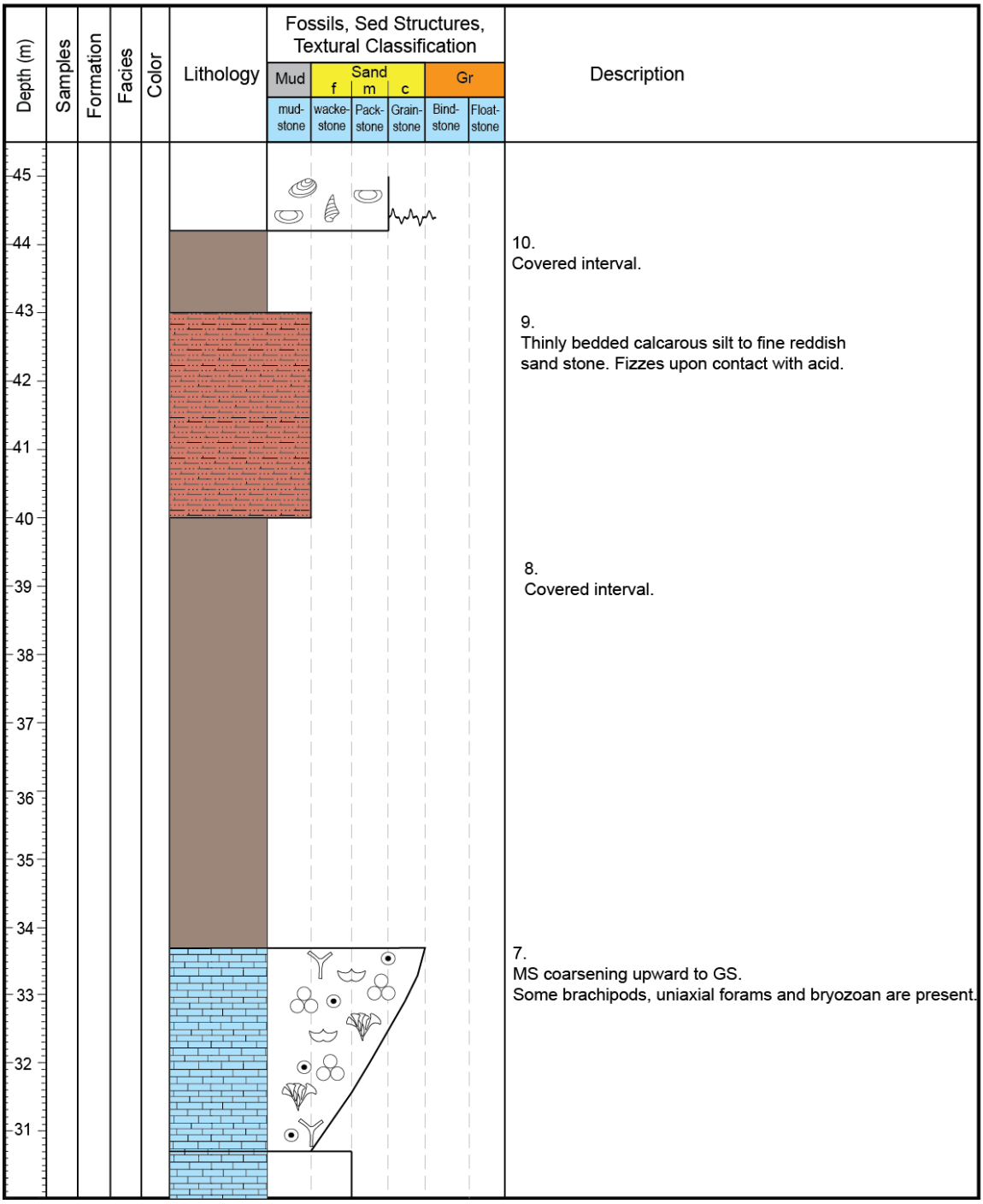

White Canyon
40.0 - 60.0 m
Location ° 0285189
4936284

Madison Formation
Mississippian
Big Horn Basin, WY

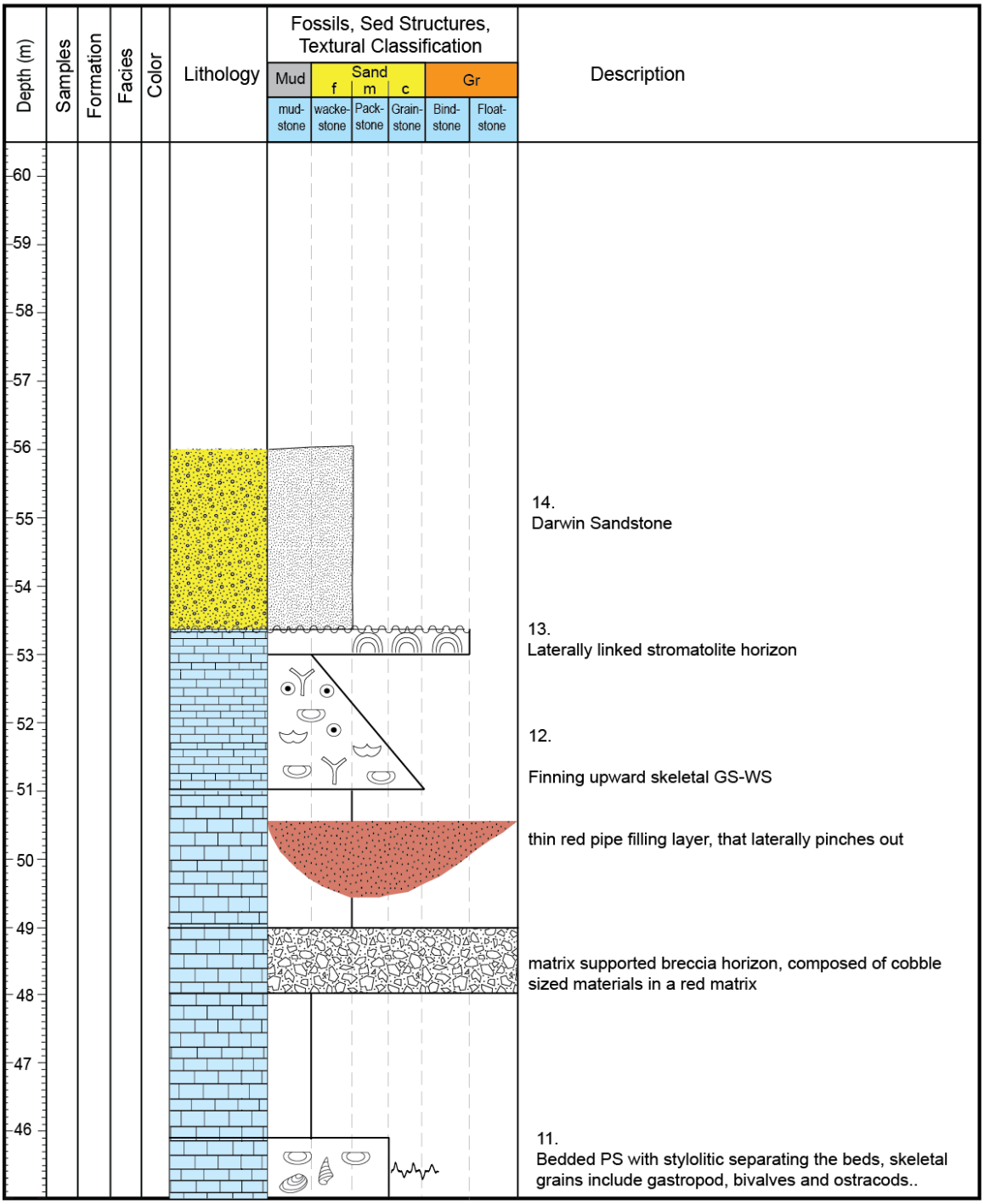

Fossil Fragments/Sedimentary Structures


Crinoids


Brachiopod


Bivalve


Gastropod


Ostracod


Corals


Echinoids


Bryozoan


Foram


Sponge/spines


Algea


Peloids


Ooids


Ooid (micritized)


Stromatolite

Diagenetic Features

Cave


Stylolite


Chert

Lithology

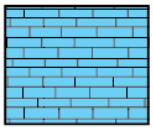
Limestone

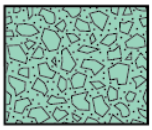
Pipe Breccia,
slightly Dolomitic in places

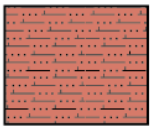
Calcareous/silty
Mudrock


Shale


Unexposed/
Inaccessible


Breccia

Table 1: Summary of raw isotopic data

Location	Depth	**δ^{13}C VPDB (‰)**	**δ^{18}O VPDB (‰)**
Medicine Lodge M1	1	-1.5	-3.2
	2	-0.2	-3.2
	2.2	-0.6	-3.8
	3.5	-1.6	-3.5
	4.2	-2.3	-4.0
	5	-2.2	-3.8
	6.5	-1.4	-2.7
	7.5	0.7	-2.4
Medicine Lodge M2	0.9	0.8	1.7
	1.1	-0.1	-3.9
	1.4	-2.7	-2.9
	1.9	-1.1	-3.9
	2.4	-1.4	-3.9
	2.9	-1.0	-3.8
	3.4	-1.1	-3.2
	3.5	-0.3	-3.0
	4.5	-0.3	-2.8
	5	-1.3	-2.7
	5.5	-1.3	-2.3
	6.5	-1.6	-2.9
	7	0.6	-2.6
	8.5	-1.8	-3.5
	9	-1.7	-3.1
	9.5	-1.9	-3.7
Medicine Lodge M3	0.3	-1.0	-2.2
	1.2	-1.5	-1.1
	1.66	-0.5	-3.4
	2.66	-2.2	-4.5
	4.16	-1.9	-3.8
	4.51	-1.6	-3.0
	5.31	-1.7	-5.5

	6.12	-1.6	-3.3
	6.81	-0.7	-3.2
	7.01	-0.7	-3.1
	7.21	-0.9	-3.3
Shell Creek Canyon	0.1	-1.5	-6.1
	0.5	-1.4	-4.7
	1	-1.5	-7.4
	2	0.2	-6.0
	3	-1.5	-5.2
	5.5	-2.9	-5.0
	5.6	-2.9	-5.2
	8	-1.2	-4.1
	9	-1.3	-4.3
	10	-1.1	-4.2
	11	-1.1	-4.5
	12	-0.9	-4.4
	14	-1.1	-4.7
	14.5	-0.3	-4.8
	15	0.0	-4.2
	16	-0.7	-4.1
	18.5	0.3	-4.0
	19	-1.3	-4.2
	20	0.4	-3.8
	24.5	-1.0	-3.6
	25	-1.4	-3.8
	25.5	-1.6	-4.3
	26.5	-1.5	-4.6
	27.5	1.0	-3.2
White Creek Canyon	6.5	-2.3	-4.0
	11	-0.9	-3.5
	13	-1.1	-4.2
	14.7	-1.1	-4.1
	15.6	-0.5	-3.8
	16.7	-1.9	-4.3
	17.2	-2.0	-3.8
	19.8	-0.7	-4.2
	21.2	-1.5	-5.0

	23.7	-2.1	-6.7
	24.7	-1.9	-4.2
	25.2	-4.0	-4.8
	25.7	1.4	-1.4
	27.2	-0.7	-4.5
	27.7	-1.7	-4.4
	28.7	-0.3	-3.5
	30.2	-1.4	-4.6
	32.7	-1.7	-5.0
	33.7	-1.3	-4.3
	44.3	-2.0	-3.6
	45.7	-1.3	-3.1
	46.9	2.2	-2.9
	48.9	-1.8	-3.0
	50.9	-1.7	-3.6
	52.4	-1.4	-3.4
	52.9	-1.2	-15.2

REFERENCES

Andrichuck, J.M., 1955, Mississippian Madison Stratigraphy and Sedimentation in Wyoming and southern Montana: Am. Assoc. Petroleum Geologist Bull., v. 39, p. 2170-2210.

Baomin, Z. and Jingjiang, L., 2009, Classification and characteristics of karst reservoirs in China and related theories. Petroleum Exploration and Development, 36 (1), pp. 12-29.

Buoniconti, M.R., 2008, The Evolution of the Carbonate Shelf Margins and Fill of the Antler Foreland Basin by Prograding Mississippian Carbonates, Northern U.S. Rockies, Unpublished Ph.D. dissertation, University of Miami, Coral Gables, pp. 456.

Buschkuehle, B. E., Hein, F.J., and Grobe, M., 2007, An Overview of the Geology of the Upper Devonian Grosmont Carbonate Bitumen Deposit, Northern Alberta, Canada: International Association for Mathematical Geology.

Choquette, P.W., and P. James, 1988, Paleokarst, Introduction, Springer-Verlag, New York, p.1-21.

Collier, A. J., and Cathcart, S. H., 1922, Possibility of Finding Oil in Laccolithic Domes South of the Little Rocky Mountains, Montana: TJ. S. Geol. Survey Bull. 736F, pp. 171-78.

Demiralin, A. S., N. F. Hurley, and T. W. Oesleby, 1993, Karst breccias in the Madison Limestone (Mississippian), Garland field, Wyoming, in R. D. Fritz, J. L. Wilson, and D. A. Yurewicz, eds., Paleokarst related hydrocarbon reservoirs: SEPM Core Workshop 18, p. 101–118.

Eliassen, A., and Talbot, M.R., 2005. Solluton collapse breccias of the Minkinfjellet and Wordiekammen Formation, central Spitsbergen, Svalbard: a large gypsum palaeokarst system. Sedimentology, v. 52, p. 775-794)

Elrick, M,. Read, J.F., 1991, Cyclic ramp-to-basin carbonate deposits, Lower Mississippian, Wyoming and Montana: a combined field and computer modeling study. Journal of Sedimentary Petrology, 61, 1194-1224.

Gutschick, R.C., and C.A., Sandberg, 1983, Mississippian continental margins of the coterminous United States, in D.J., Stanley and G.T. Moore, eds., The Shelf break: Critical interface on continental margins, SEPM Special Publications no. 33, p. 79-96.

Katz, D.A., Eberli, G.P., Swart, P.K., Smith, L.B. Jr., 2006. Tectonic-hydrothermal brecciation associated with calcite precipitation and permeability destruction in Mississippian carbonate reservoirs, Montana and Wyoming: Am. Assoc. Petroleum Geologists Bull., v. 90, Special Issue: Hydrothermally Altered Carbonate Reservoirs, p.

1803-1841.

Katz, D.A., 2008. Early and Late Diagenetic Processes of Mississippian Carbonates, Northern U.S. Rockies. Ph.D. dissertation. University of Miami, Miami, Florida. 444 pp.

Kendall, A.C., 1992, Evaporites, in R.G. Walker and N.P. James, eds., Facies models: Response to sea-level change: St. Johns, Newfoundland, Geological Association of Canada, p. 375-409.

Kerans, C., 1988, Karst-Controlled Reservoir Heterogeneity in Ellenburger Group Carbonates of West Texas: AAPG Bulletin, v. 72, p. 1160– 1183.

Kerans, C. 1989, Karst-Controlled Reservoir Heterogeneity and an Example from the Ellenburger Group (Lower Ordovician) of West Texas: Report of Investigations No. 186, Texas Bureau of Economic Geology,. 40 p.

Kloss, T.T., 2011, Evolution of a regionally extensive evaporite removal paleokarst complex: Mississippian Madison Group, Wyoming, unpublished Master's thesis, University of Texas, Austin, TX, 117 p.

Lohmann, K. C., 1988, Geochemical patterns of meteoric diagenetic systems and their application to studies of paleokarst, in N. P. James and P. W. Choquette, eds., Paleokarst: Berlin, Springer-Verlag, p. 58–80.

Loucks, R. G., and P. K. Mescher, 1997, Interwell scale architecture, heterogeneity, and pore-network development in paleocave reservoirs: Dallas Geological Society and SEPM Field Trip 11 Guidebook, unpaginated.

Loucks, R. G., 1999, Paleocave carbonate reservoirs: origins, burial depth modifications, spatial complexity, and reservoir implications: AAPG Bulletin, v. 83, p. 1795– 1834.

Mckerrow, W.S., and C.R. Scotese, 1990, Revised world maps and introduction, in W.S. McKerrow and C.R. Scotese, eds., Paleozoic paleogeography and biogeography: Geological Society Memoir 12, p. 1-24.

Purdy, E.G. and Waltham, D., 1999. Reservoir implications of modern karst topography. AAPG Bulletin, **83**, pp. 1774-1794.

Rose, P.R., 1976. Mississippian carbonate shelf margins, western United States. In: Hill, J. G. (Ed), Geology of the Cordilleran Hingeline. Denver, Rocky Mountain Association of Geologists, pp. 135-151.

Saller, A.H., Dickson, J.A.D. and Matsuda, F., 1999. Evolution and distribution of porosity associated with subaerial exposure in upper Paleozoic platform limestones, West Texas. AAPG Bulletin, **83**, pp. 1835-1854.

Sandberg, C.A., Klapper, G., 1967. Stratigraphy, age, and significance of the Cottonwood

Canyon Member of the Madison Limestone in Wyoming and Montana. United States Geological Survey Bulletin 1251-B, 70.

Sando, W. J., 1967. Madison Limestone (Mississippian) Wind River, Washakie, and Owl Creek Mountains, Wyoming. AAPG Bulletin 51, 529-557.

Sando, W.J., 1974. Ancient solution phenomena in the Madison Limestone (Mississippian), east flank of Bighorn Mountains, Wyoming. In: Laudon, R.B. m(Ed.), Geology and Energy Resources of the Powder River Basin, Wyoming Geological Association 28th Annual Field Conference Guidebook, p. 45-51. 136

Sando, W. J., M. Gordon Jr., and J. T. Dutro Jr., 1975, Stratigraphy and geologic history of the Amsden Formation (Mississippian and Pennsylvanian) of Wyoming: U.S. Geological Survey Professional Paper 858-A, p. 78.

Sando, W. J., 1976, Mississippian history of the northern Rocky Mountains region. U.S. Geological Survey Journal of Research 4, 317-338.

Sando, W. J., C. A. Sandberg, and R.C. Gutschick, 1981, Stratigraphic and economic significance of Mississippian sequence at North Georgetown Canyon, Idaho: AAPG Bulletin, v. 65, p. 1433-1443.

Sando, W. J., 1985. Revised Mississippian timescale, western interior region, coterminous United States. U.S. Geological Survey Bulletin, 1605-A [1986], pp. A15- A26

Sando, W. J., 1988, Madison Limestone (Mississippian) paleokarst: a geologic synthesis, in N. P. James and P. W. Choquette, eds., Paleokarst: Berlin, Springer-Verlag, p. 256–277.

Seemann, U., Pumpin, V.F. and Casson, N., 1990. Amposta oil field. AAPG Treatise of Petroleum Geology, Atlas of Oil and Gas Fields, **A-017**, pp. 1-20.

Sieverding, J.L., and Harris, P.M., 1991. Mixed carbonates and silicilastics in a Mississippian paleokarst setting, southwestern Wyoming thrust belt, In: Lomando, A.J. and Harris, P.M. (Eds) SEPM: Mixed Silicilastics Sequence, v 15, p. 541-568.

Smith, L.B. Jr., Eberli, G.P., Sonnenfeld, M 2004. Sequence-stratigraphic and Paleogeographic Distribution of Reservoir-Quality Dolomite, Madison Formation, Wyoming and Montana, In: Integration of Outcrop and Modern Analogs in Reservoir Modeling: AAPG Memoir 80, pp. 67-92.

Sonnenfeld, M.D., 1996a. Sequence evolution and hierarchy within the lower Mississippian Madison Limestone of Wyoming, In: Longman, M.W., Sonnenfeld, M.D. (Eds.), Paleozoic Systems of the Rocky Mountain Region. Society for Economic Paleontologists and Mineralogists (Society for Sedimentary Geology) Rocky Mountain Section, pp. 165-192.

Sonnenfeld, M.D., 1996b. An integrated sequence stratigraphic approach to reservoir characterization of the Lower Mississippian Madison Limestone, emphasizing Elk Basin field, Bighorn Basin, Wyoming. Unpublished Ph.D. dissertation. Colorado School of Mines, Golden, Colorado.

Tinker, S. W., and D. H. Mruk, 1995, Reservoir characterization of a Permian giant: Yates field, west Texas, in E. L. Stoudt and P.M. Harris, eds., Hydrocarbon reservoir characterization; geologic framework and flow unit modeling: SEPM Short Course 34, p. 51–128.

Trexler, J. H., Cashman, P. H., Cole, J.C., Snyder, W.S., Tosdal, R.M., and Davydov, V.I., 2010. Widespread effects of middle Mississippian deformation in the Great Basin of western North America. Geological Society of America Bulletin, 2003, pp. 1278-1288

Vail, P.R., Mitchum, R.M., Thompson S., III., 1977. Seismic stratigraphy and global changes of sea level, Part 4: Global cycles of relative changes in sea level. In: Payton, C.E. (Ed.), Carbonate Sequence Stratigraphy-Applications to Hydrocarbon Exploration. American Association of Petroleum Geologists Memoir 26, pp. 83-97.

Veevers, J.J., Powell, C.M., 1987. Late Paleozoic glacial episodes in Gondwanaland reflected in transgressive-regressive depositional sequences in Euramerica. Geological Society of America Bulletin 98, pp. 179-196.

Viniegra-O, F., and C. Casstillo-Tejero, 1970, Golden Lane fields, Veracruz, Mexico, in M. T. Halbouty, ed., Geology of giant petroleum fields: AAPG Memoir 14, p. 309–325.

Warren, J., 1999. Evaporites. Their evolution and economics. Blackwell Science, 438 p.

Wright, V. P., 1991, Palaeokarst: types, recognition, controls and associations, in V. P. Wright, M. Esteban, and P. L. Smart, eds., Palaeokarsts and palaeokarstic reservoirs: Postgraduate Research for Sedimentology, University of Reading, PRIS Contribution